A Model for Formation of Dust, Soil and Rock Coatings on Mars: Physical and Chemical Processes on the Martian Surface

Janice L. Bishop[1], Scott L. Murchie[2], Carlé M. Pieters[3], and Aaron P. Zent[4]

[1]SETI Institute/NASA-ARC, MS-239-4, Moffett Field, CA 94035 (jbishop@mail.arc.nasa.gov),

[2]Applied Physics Lab, Laurel, MD, 20723,

[3] Brown Univ. Box 1846, Providence, RI 02912,

[4]NASA-ARC, MS-245-3, Moffett Field, CA 94035.

Running title: Mars Soil and Rock Alteration Model

Abstract. This model is one of many possible scenarios to explain the generation of the current surface material on Mars using chemical, magnetic and spectroscopic data from Mars and geologic analogs from terrestrial sites. One basic premise of this model is that the dust/soil units are not derived exclusively from local rocks, but are rather a product of global, and possibly remote, weathering processes. Another assumption in this model is that there are physical and chemical interactions of the atmospheric dust particles and that these two processes create distinctly different results on the surface. Physical processes distribute dust particles on rocks and drift units, forming physically-aggregated layers; these are reversible processes. Chemical reactions of the dust/soil particles create alteration rinds on rock surfaces and cohesive, crusted surface units between rocks, both of which are relatively permanent materials. According to this model the dominant components of the dust/soil particles are derived from alteration of volcanic ash and tephra, and contain primarily nanophase and poorly crystalline ferric oxide/oxyhydroxide phases as well as silicates. These phases are the alteration products that formed in a low moisture environment. These dust/soil particles also contain a smaller amount of material that was exposed to more water and contains crystalline ferric oxides/oxyhydroxides, sulfates and clay silicates. These components could have formed through hydrothermal alteration at steam vents or fumeroles, thermal fluids, or through evaporite deposits. Wet/dry cycling experiments are presented here on mixtures containing poorly crystalline and crystalline ferric oxides/oxyhydroxides, sulfates and silicates that range in size from nanophase to 1-2 μm diameter particles. Cemented products of these soil mixtures are formed in these experiments and variation in the surface texture was observed for samples containing smectites, non-hydrated silicates or sulfates. Reflectance spectra were measured of the initial particulate mixtures, the cemented products and ground versions of the cemented material. The spectral contrast in the visible/near-infrared and mid-infrared regions is significantly reduced for the cemented material compared to the initial soil, and somewhat reduced for the ground, cemented soil compared to the initial soil. The results of this study suggest that diurnal and seasonal cycling on Mars will have a profound effect on the texture and spectral properties of the dust/soil particles on the surface. The model developed in this study provides an explanation for the generation of cemented or crusted soil units and rock coatings on Mars and may explain albedo variations on the surface observed near large rocks or crater rims.

2

1. Introduction and Background

This project includes analysis of the spectral, chemical and magnetic data from Mars Pathfinder soil together with analog materials and the products of laboratory alteration experiments in order to describe possible mechanisms for the formation of drift, cemented soil and rock coatings on Mars. Soil analog mixtures have been prepared, characterized and tested through wet/dry cycling experiments for changes in binding and spectroscopic properties that are related to what could be expected for cemented soil units on Mars. Hydrothermal and solfataric alteration of volcanic tephra frequently produces reactive sulfate species that may attack the surfaces of dust particles and rocks to form cemented soil units and rock coatings. This idea is pursued here. Recent magnetic, chemical, spectral and imaging data from Mars Pathfinder suggest that surface alteration and/or weathering has taken place on Mars and that there may be coatings on the rocks resulting from these processes [*Madsen et al.*, 1999; *McSween et al.*, 1999; *Bell et al.*, 2000]. Combining these results from Pathfinder with results from laboratory studies [e.g. *Bishop et al.*, 1995, 1998a; *Bishop and Murad*, 1996; *Banin et al.*, 1997; *Morris et al.*, 1997, 1998, 2000, 2001] provides the clearest picture of the mineralogy and potential alteration processes on Mars.

1.1. Composition of Martian Surface Rocks and Soils

Characterization of the composition of Mars has been approached through telescopic observations as well as instruments on landers and orbiters. The spectral properties of bright and dark regoliths on Mars have been summarized by *Soderblom* [1992] and *Roush et al.* [1993] and of alteration minerals on Mars by *Bell* [1996]. Thermal IR analyses of Mars have shown that global rock compositions are basaltic to andesitic [*McSween et al.*, 1999; *Bandfield et al.*, 2000; *Christensen et al.*, 2000b] and that a large region of gray hematite is present [*Christensen et al.*, 2000a].

The MPF site is located in a transition region between typical bright and dark regions [*Golombek et al.*, 1997]. The chemical and mineralogical compositions of the rocks near the Mars Pathfinder (MPF) lander indicate that they are andesitic-basaltic and locally derived, and that many rocks are covered with alteration rinds [*McSween et al.* 1999]. Analysis of the Pathfinder soil units has shown that they are chemically and mineralogically distinct from the

rocks, and that they may contain goethite, maghemite or other iron oxyhydroxides [*Bell et al.* 2000], but do not show the expected evidence for crystalline hematite based on previous telescopic measurements of Mars [*Bell et al.*, 1990]. Chemical mixing models have shown that simple soil-rock mixing scenarios are inadequate to explain the chemical composition of the Martian rocks and soils [*McLennan*, 2000; *McSween and Keil*, 2000] and that the global dust on Mars resulted from weathering of basaltic rather than felsic rocks [*McLennan*, 2000; *McSween and Keil*, 2000; *Morris et al.*, 2000].

The magnetic tests on the Viking and MPF landers indicated the presence of a magnetic component intimately mixed with non-magnetic components, such as silicates, in the dust/soil particles [*Hargraves et al.*, 1977; *Pollack et al.*, 1977; *Hviid et al.*, 1997; *Madsen et al.*, 1999]. Saturation magnetization, J_s, has been estimated from the magnetic experiments on the MPF lander and depends on the assumed particle density. *Madsen et al.* [1999] estimate J_s at 4 ± 2 Am^2/kg, while *Morris et al.* [2001] estimate J_s at 2.5 ± 1.5 Am^2/kg. A few wt.% Fe_2O_3 as maghemite [*Hargraves et al.*, 1977; *Hviid et al.*, 1997; *Madsen et al.*, 1999] and magnetite /titanomagnetite [*Pollack et al.*, 1977; *Morris et al.*, 2000] have both been proposed as the magnetic minerals present in the Martian dust/soil based on these data, leaving the bulk of the iron in the Martian dust/soil in ferrous silicates or non-magnetic (probably nanophase) ferric oxides/oxyhydroxides.

1.2. IMP Spectra

The Imager for Mars Pathfinder (IMP) has produced numerous spectra of specific soil units near the mouth of the Ares and Tiu flood channels [*Smith et al.*, 1997]. Spectral analyses of laboratory soil analog materials and several soil units measured by the IMP showed that there are specific differences in the soils observed by Pathfinder that are attributed to differences in mineralogy and composition of the soils [e.g. *Bishop et al.*, 1998d; *Bell et al.*, 2000]. Specifically, many of the soils are characterized by a smooth upward slope from 0.5 to 0.7 μm and a broad maximum near 0.75 μm. Some soil units have a stronger shoulder feature near 0.6 μm and some exhibit a weak, broad band near 0.9 μm. Variations in the chemical abundances of these soils indicate a good correlation of wt.% SO_3 with the red/blue reflectance ratios [*Bridges et al.*, 2001]. This suggests that the ferric minerals responsible for the reflectance maximum near

0.75 µm are correlated with sulfates in the soils. Ratios of numerous spectral parameters have been performed and are summarized by *Bell et al.* [2000].

Spectral analyses, including determination of the T_1 and T_2 band centers and calculation of crystal field parameters, of IMP soils and soil analogs enabled separation of groups of iron oxyhydroxide-silicate aggregates according to redox conditions and sulfate content [*Bishop et al.*, 1998d]. This study showed that the spectral character of many of the Martian soils measured by IMP contains a reflectance maximum near 0.8 µm that is consistent with nanophase ferric oxides/oxyhydroxides. It also demonstrated variability in the shape of the 0.6 µm shoulder feature that would be consistent with variable abundance of a sulfate (e.g. schwertmannite, jarosite) or goethite. If magnetite is also a soil component it could be responsible for weakening the ~0.9 µm absorption characteristic of ferric oxides. Preliminary analyses indicate that adding the ~6% maghemite estimated for the IMP soils [*Hviid et al.* 1997; *Madsen et al.* 1999] would not greatly alter the spectral character of these samples. Natural soils containing magnetite are darker than otherwise similar samples, exhibit a weaker 0.9 µm band and a broad, shallow absorption centered near 1.5 µm [*Scheinost et al.*, 1998; *Morris et al.*, 2000]. *Morris et al.* [2000] further observed that the finest size fractions of altered tephra become darker with increasing magnetic susceptibility due to the presence of magnetic Fe,Ti-oxides.

1.3. Terrestrial Alteration of Volcanic Tephra/Ash

Recent studies of the fine-grained fractions of volcanic material indicate that there are multiple kinds of alteration processes taking place: palagonitic, pedogenic or solfataric alteration of volcanic tephra, ash or lava [e.g. *Morris et al.*, 1993, 1996, 2000; *Bishop et al.*, 1998a, 2001; *Schiffman et al.*, 2000, 2001]. Long-term palagonitic weathering of volcanic tephra in a dry environment have been contrasted with the more rapid and/or intense sulfatetic or solfataric alteration in the vicinity of steam vents and cinder cones [*Bishop et al.*, 1998a]. Palagonitic weathering involves hydration and vitrification of basaltic glass to form fine-grained and poorly-crystalline ferric oxides/oxyhydroxides and silicate phases under low temperature and low moisture conditions, with the formation of smectite and serpentine clay minerals under higher temperature and higher moisture conditions [e.g. *Bates and Jackson*, 1984; *Bishop et al.*, 2001; *Morris et al.*, 2001; *Schiffman et al.*, 2001]. The solfatarically altered tephra often contain significant amounts of crystalline iron oxides/oxyhydroxides and jarosite/alunite, while the

palagonitic tephra tend to contain poorly crystalline and/or nanophase minerals. A bright red tephra sample (250) collected from a cinder cone in the Haleakala crater basin is particularly interesting because it is extremely fine-grained (substantial fraction of <2 μm particles), magnetic and contains both jarosite and iron oxides/oxyhydroxides [*Bishop et al.*, 1998a]. Additional jarositic tephra from Mauna Kea have been analyzed that do not contain iron oxides [*Morris et al.*, 1996] and from the Kilauea region that contain a variety of iron oxides/oxyhydroxides including hematite and goethite [*Morris et al.*, 2000]. *Calvin et al.* [1999] also presented reflectance spectra of selected sulfate minerals formed in terrestrial steam vents or fumeroles. Potential factors contributing to ferric oxide/oxyhydroxide formation along with jarosite and other sulfates in such soils include the temperature and composition of the volcanic gases, duration of hydrothermal exposure, and oxidation following hydrothermal alteration.

Palagonitic alteration of glassy basalts and andesites has been characterized using a variety of geochemical and mineralogical techniques [e.g. *Colman*, 1982; *Staudigel and Hart*, 1983; *Nesbitt and Young*, 1984; *Fisher and Schminke* 1984]. These studies have shown that volcanic glass and olivine are generally the least stable components of basaltic deposits, while Fe,Ti-oxides are the most resistant to alteration. According to these and other studies, the typical low temperature alteration products of mafic volcanic rocks are a mixture of short-range ordered aluminosilicates (e.g. allophane and imogolite), amorphous iron oxide/oxyhydroxides, and poorly crystalline and crystalline clay minerals (including smectite and kaolinite). A recent study of numerous palagonitically altered Hawaiian tephra samples observed Fe,Ti-oxides and nanophase crystalline iron oxyhydroxides, but did not find evidence of phyllosilicates [*Morris et al.* 2000]. Palagonitization and formation of weathering rinds on basalts and andesites are also accompanied by large reductions in Ca, Mg, Na and K, depletion in Si, oxidation of the Fe, and incorporation of water [e.g. *Fisher and Schminke*, 1984].

Partially palagonitized Mauna Kea ash has recently been proposed by *Morris et al.* [2001] as a potential Martian dust analog material. *Morris et al.* [2001] identified tiny magnetite grains (5-150 nm) imbedded in an altered glassy silicate matrix, where the magnetite grains formed at the time of glass formation and contain variable amounts of Ti, and the silicate glass has altered to form allophane and nanophase iron oxides/oxyhydroxides but not phyllosilicates. Such poorly altered volcanic ash particles could fit into our model if they were exposed to solfataric alteration

6

(e.g. cinder cones, fumeroles) to form sulfate minerals or admixed with sulfates formed via evaporitic or other processes.

1.4. Possible Alteration Scenarios on Mars

Our model is based upon mixing and distribution of dust/soil components and chemical reaction of selected species in the dust/soil particles. The aeolian processes invoked for our model are similar to patterns of dust deposition and removal described by *McSween et al.* [1999] in order to explain variable rock coatings. Our model is distinct from others presented recently including "acid-fog" weathering [*Banin et al.*. 1997] and hydrothermal fluids from geothermal hot springs [*Newsom et al.*, 1999]. Other alteration scenarios that have been described as potentially contributing to soil formation on Mars include chemical alteration of martian meteorite-like rocks [*Dreibus et al.*, 1998; *Brückner et al.*, 1999; *Wänke*, 1999], partial palagonitization of volcanic ash [*Morris et al.*, 2001] and physical alteration of rocks [*Bridges et al.* 1999; *Ruff and Christensen*, 1999]. Impacts have also been suggested as mechanisms of producing glassy alteration products containing ferric oxides on Mars [*Morris et al.*, 1995; *Schultz and Mustard*, 1998; *Minitti et al.*, 2000; *Yen*, 2001].

2. Model Outline

A model was developed that describes potential mechanisms of rock coating and duricrust formation on Mars [*Bishop et al.*, 1999]. We acknowledge that the data available at this time are insufficient for unique determination of any given surface model and we are proposing this as one of many possibilities for consideration. This model states that (1) the ~2 µm sized "dust" particles suspended in the atmosphere on Mars are compositionally similar to the "soil" covering the surface of rocks and the ground in between rocks, (2) physical processes (e.g. wind, dust devils) primarily govern distribution, aggregation and disaggregation of the dust, soil and dust layers on rocks, and (3) chemical processes (e.g. chemical reactions of the sulfates with the ferric oxide and silicate surfaces in the presence of water and/or redox reactions of Fe^{2+}/Fe^{3+}) are primarily responsible for the formation of rock coatings and duricrust and that once formed, these chemical layers cannot be simply disaggregated by the wind. This model has been refined and expanded into the present form.

In this model volcanic steam vents and hydrothermal activity associated with volcanism are primarily responsible for the production of crystalline, Fe and S-bearing minerals such as hematite, maghemite/ magnetite, and jarosite/alunite. Evaporite deposits may be another source of sulfates and salt minerals. These minerals form in high concentrations ($\geq$ half of the composition of the altered ash) in specific locations – abundant, yet not ubiquitous. In contrast, palagonitic alteration of volcanic ash is more common and prevalent, and results in nanophase Fe oxide phases, poorly crystalline clays and/or protoclays (e.g. allophane and immogolite), poorly crystalline grains of feldspar and pyroxene, and tiny glass particles. Aeolian mixing of these two alteration materials produces a non-homogenous but regionally similar, fine-grained material. This explains the subtle differences in dust/soil composition measured at the Viking and Pathfinder lander sites [*Clark et al.*, 1982; *Bell et al.*, 2000; *Foley et al.*, 2001].

2.1. Physical Interactions

Mars sustains periodic large-scale dust storms that can vary in size and intensity up to complete global coverage. A persistent background optical depth of 0.3-1.0 was measured at the Viking Lander sites for visible wavelengths [*Pollack et al.*, 1979]. Wind tails have been observed at the Viking and MPF landing sites and suggest that aeolian processes have been active [*Arvidson et al.*, 1989; *Greeley et al.*, 1992, 1999]. Localized dust devils have been identified on Mars in Viking images [*Thomas and Gierasch*, 1985], in Pathfinder surface images [*Metzger et al.*, 1999] and in MOC images [*Edgett and Malin*, 2000]. A mean dust particle size at the MPF lander site of ~1.6 µm in radius was determined from pressure changes and calculations of dust loading [*Smith and Lemmon*, 1999; *Tomasko et al.*, 1999], which was also observed at the Viking sites [*Pollack et al.*, 1995]. Evidence for aeolian distribution of dust particles on Mars has been observed in nearly every measurement/experiment suggesting that it is a pervasive surface process [*Greeley et al.*, 1999]. *Metzger et al.* [1999] estimated that a dust devil located on the southern flank of the South Twin Peak had a vortex 14 m wide by 230 m high and a ground speed of 0.5 m/s.

The idea that these local dust devils could be disaggregating and suspending soil particles and redistributing them as 1-3 µm sized dust particles was presented by *Bishop and Smith* [1999]. Here it is further suggested that there is a reversible interaction between these dust particles suspended in the atmosphere and the soil particles covering the surface. As long as the particles

are kept in motion and are prevented from forming chemical bonds, they can be readily disaggregated and/or redistributed. A diagram of this process is shown in Figure 1, where particles can be transformed from atmospheric dust to drift and from atmospheric dust to physical rock coatings and back to dust again with the next dust devil or dust storm.

According to our model these dust particles settle on the rocks to form physical dust coatings (a thin layer sprinkled on the surface) and cover the surfaces in between rocks to form drift deposits. The physical coatings and drift units in this model are compositionally similar to the atmospheric dust particles; the primary difference is that the drift deposits and rock coatings contain larger aggregates of dust particles, held together by electrostatic or physical forces. Spectral and chemical evidence from Mars Pathfinder revealed than many of the surface soil units are compositionally similar; spectral differences for many units are thought to be due to grain size and compaction [*Bell et al.*, 2000]. Although the spectral properties of dust particles suspended in the atmosphere near MPF are different from spectral properties of drift deposits, especially in the blue wavelengths [*Thomas et al.*, 1999; *Bell et al.* 2000], this is not necessarily inconsistent with our model. The spectral properties of suspended particles are not well characterized because they are difficult to measure and would include scattering through greater distances than in dust deposited on a surface.

McSween et al. [1999] suggest that coatings of drift material on rocks near the MPF site may be responsible for some of the rock spectral observations based on laboratory studies [*Fischer and Pieters*, 1993; *Johnson*, 1999; *Morris et al.*, 2000]. Rock coatings were suggested in earlier studies as well to explain the Viking lander multispectral observations [*Adams et al.*, 1986; *Guinness et al.*, 1987]. *Fischer and Pieters* [1993] showed that an optically thin coating of fine-grained ferric particles on a dark neutral substrate (e.g. basalt) induces an increase in the visible/NIR region reflectance and the red/blue ratio, and produces ferric absorption bands. Thin coatings of fine-grained, altered volcanic ash were also observed to influence the mid-IR reflectance and emission spectra of basaltic rocks [*Crisp and Bartholomew*, 1992; *Johnson*, 1999]. *Crisp and Bartholomew* [1992] found that a layer 25 μm deep of fine-grained ash on basalt suppressed the silicate bands near 10 and 19 μm by about 50%. Based on these studies a layer as thin as a few microns is sufficient to induce measurable changes in the visible/NIR and mid-IR spectral properties of basalts.

2.2. Chemical Interactions

In contrast to physical aggregates of particles, chemical interactions of dust particles in the soil or on rock coatings form more permanent, cemented products. These are shown as irreversible pathways in Figure 1. This process requires the formation of chemical bonds. These bonds can be broken again, but this would require a more active process than simply a dust devil. The processes creating ventifacts on rock surfaces [*Bridges et al.*, 1999], for example, would be sufficient to remove rock varnishes. Shown in Figure 2 are examples of the kinds of bonds that may be formed when the physical dust layer is transformed into a chemically bound cemented soil or rock varnish. Sulfates or ferric oxides/oxyhydroxides are likely to be the binding agents in these chemically bound materials.

Sulfate species are particularly reactive because of their polar nature, as are Fe^{3+} bearing phases because they readily accept electrons. For these reasons dust/soil particles containing ferric oxides/oxyhydroxides and jarosite/alunite would be particularly reactive. If these dust particles are allowed to remain undisturbed on the surfaces of rocks sufficiently long to enable chemical reactions between the ferric, sulfate and salt species and the primary rock minerals, then alteration rinds would form that would be resistant to dust devils or wind storms. Only minimal water is required for these chemical reactions (given long time scales), and this would be provided via atmospheric water ice particles. Evidence for these exists through diurnal variations in the atmosphere observed using data from the Viking orbiters [*Farmer et al.*, 1977], telescopic observations [*Sprague et al.*, 1996] ISM on the Russian orbiter [*Titov et al.*, 1995] and MPF lander [*Smith and Lemmon*, 1999].

Of course chemical reactions would have progressed much faster on Mars in the presence of liquid water. Although there is no direct evidence of liquid water on Mars, hypotheses for liquid water abound. *Carr* [1981] has suggested that abundant flowing water best explains the many runoff and outflow channels depicted in Viking images of Mars. Analyses by *Baker et al.*, [1991], *Clifford* [1993] and *Parker et al.* [1993] support the presence of aqueous processes and perhaps sedimentary deposits and an ancient ocean on Mars. Recently observed erosional features on Mars have been explained by groundwater seepage and surface runoff [*Malin and Edgett*, 2000b] and sedimentary deposits [*Malin and Edgett*, 2000a]. Although non-aqueous explanations have also been submitted for these Martian surface features [e.g. *Hoffman*, 2000;

Musselwhite et al., 2001], a number of scenarios involving aqueous and subaqueous processes on Mars are possible, and consideration of potential chemical alteration mechanisms are warranted.

3. Laboratory Alteration Studies

A set of laboratory experiments was designed to demonstrate the dust-soil-cemented soil portion of this model. Rock coating experiments are part of a future study. Two soil analog mixtures were prepared that are a combination of synthetic and natural materials. The goal in designing these two samples was not to exactly recreate the soil chemistry measured by MPF, but rather to prepare analog materials that are, in general, consistent with the chemical, magnetic and spectroscopic properties of the Martian soil to be used in experiments testing the feasibility of soil alteration reactions on Mars.

3.1. Mixture Samples

Samples for this study were prepared by combining powders of sulfate-bearing volcanic soils and magnesium sulfate with either iron oxyhydroxide-montmorillonite aggregates or fine-grained altered volcanic ash. The sulfate-bearing soils are examples of products forming from solfataric alteration and the magnesium sulfate is an example of what could form through an evaporite deposit on Mars. The first mixture (Mix-1) contains 70 wt.% of sample jb11 (synthetic iron oxyhydroxide-montmorillonite aggregate soil, from *Bishop et al.* [1995]), 10 wt.% of sample jb250 (sulfate-bearing volcanic soil, collected on the rim of a cinder cone, Haleakala crater basin, from *Bishop et al.* [1998a]), 10 wt.% of sample 182 (sulfate-bearing volcanic soil, collected near an active steam vent, Santorini, from *Bishop et al.* [1998a]), and 10 wt.% of hydrated magnesium sulfate ($MgSO_4 \cdot 7H_2O$ from Fisher Scientific). The second mixture (Mix-2) contains 70 wt.% of sample jb248 (fine-grained altered volcanic ash, Haleakala crater basin, from *Bishop et al.* [1998a]), and 10 wt.% each of the other three samples as described for Mix-1. The iron oxyhydroxide-montmorillonite aggregate soil was produced in the lab by exchanging the Ca/Na interlayer cations with Fe, which then further reacts to form oxyhydroxides [*Bishop et al.* 1995]. This is a chemical mixture of nanophase to micron-sized particles bound together. The volcanic soil samples included in these mixtures contain a variety of poorly crystalline, altered phases including nanophase ferric oxyhydroxide particles, fine-grained sulfates, and

silicates. These soil samples include both chemical and physical mixing of nanophase to micron-sized particles. Shown in Figure 3 is an example of how these chemically and physically mixed particles may appear. All endmembers were dry sieved to <45 μm prior to mixing.

Chemical compositions were measured previously of the Fe-montmorillonite and volcanic soil endmembers. The approximate chemical composition of each mixture was determined by summing the relative proportions of the mixture components. This is given in Table 1. The chemical composition for the magnesium sulfate used is based on the assumption that this salt was uncontaminated. The magnetic susceptibility of the mixtures was measured as in previous studies [e.g. *Morris et al.* 2000, 2001] and found to be on the order of what was observed for the dust at the MPF site, and slightly higher for Mix-2 than for Mix-1 (R.V. Morris, pers. comm.).

3.2. Reflectance Spectroscopy

Visible-infrared reflectance spectra were measured as described in previous experiments [*Pieters*, 1983; *Bishop et al.*, 1995]. Bidirectional visible/near-infrared spectra were measured relative to Halon under ambient conditions at the Reflectance Experiment Laboratory (RELAB) at Brown University. Biconical infrared reflectance spectra were measured relative to a rough gold surface using a Nicolet 740 Fourier transform interferometer (FTIR) in a H_2O- and CO_2-purged environment. Composite, absolute reflectance spectra were prepared by scaling the FTIR data to the bidirectional data near 1.2 μm.

3.3. Hydration/dehydration Cycling Experiments

Wet/dry cycling experiments were performed on four samples: the two new mixtures described here plus each of the dominant endmembers for these mixtures. The samples were exposed to repeated cycles of dehydration and re-hydration in the laboratory. The samples were hydrated by adding about 500 μl of distilled, deionized water to the sample surface; re-hydration was performed by adding 100-300 μl H_2O. Dehydration was performed by drying the samples in air, in a desiccator and by heating at low temperature in an oven. These experiments were performed by pouring the freshly dry sieved (fluffy) mixtures into sample dishes 10 mm in diameter, where the samples remained for the duration of the experiment. The specific hydration history for the samples in this study included several steps: dehydration in a desiccator, hydration with H_2O, drying in air, dehydration in a desiccator, re-hydration with H_2O, dehydration in a

desiccator. tapping of the dishes in order to break the surface tension of the crust, re-hydration with H_2O, heating in an oven for 1 hour at 50 °C. The degree of moisture used in these experiments is more representative of past climatic regimes on Mars than the current one; however, the crust-formation trends should be similar. The timescale for crust formation would vary depending on available water and would require much longer using actual diurnal water variation levels and would thus be impractical for lab experiments.

4. Results – Composition and Spectroscopic Properties of Mixtures

Shown in Figures 4 and 5 are visible/NIR and mid-IR reflectance spectra of the two new mixtures and endmember components used in this study. The spectrum of the hydrated magnesium sulfate ($MgSO_4 \cdot 7H_2O$) is brightest in the visible/NIR region and the altered volcanic soils are the darkest. Soil Mix-1 (364) is darker than its dominant iron oxyhydroxide-montmorillonite endmember (Fe-mont, 11) and both the reflectance maximum near 0.75 μm and minimum near 0.88 μm are shifted towards shorter wavelengths from those of the iron oxyhydroxide-montmorillonite sample. Also the characteristic montmorillonite bands near 1.42, 1.91 and 2.20 μm are weaker and broader in spectra of soil Mix-1. Soil Mix-2 (365) is less noticeably changed from its dominant palagonitically altered volcanic soil endmember (248). Although the spectral features for soil Mix-2 are weak in this region, soil Mix-2 exhibits more pronounced features than palagonitic soil 248, including: the reflectance maximum near 0.78 μm, the reflectance minimum near 0.86 μm, and phyllosilicate absorptions near 1.4, 1.9 and 2.2 μm. Hydrated magnesium sulfate also has narrow bands in this region near 1.44 and 1.94 μm, as well as broad bands near 2.9-3.1 and 4.4-4.6 μm. Although the hydrated magnesium sulfate makes up only 10 wt.% of each mixture these are strong absorption features, so this component is likely contributing to the NIR spectral properties of the mixtures.

The mid-IR spectra are shown in Figure 5 in terms of wavenumber, in cm^{-1}, in order to best show the spectral features and facilitate comparison with Thermal Emission Spectrometer (TES) spectra. The hydrated magnesium sulfate spectrum has the strongest contrast in this region and the altered volcanic soils exhibit the least spectral contrast. All of the spectra have a water band near 1630-1650 cm^{-1} (~6.1 μm). The magnesium sulfate powder spectrum contains a strong band near 950 cm^{-1} (~10.5 μm) as shown in Figure 5 which is shifted to 1150 cm^{-1} (~8.7 μm) for cemented magnesium sulfate [*Cooper and Mustard*, 2001b]. Silicate bands are observed near

13

1075-1150 cm^{-1} (~9 μm) and 470-540 cm^{-1} (~20 μm) for Mix-1, the iron oxyhydroxide-montmorillonite (11) and the Santorini soil (182).

Comparison of the chemistry, mineralogy and spectral properties of the two soil mixtures prepared for this study shows that although they each are a mixture of related components, there are major differences. Mix-1 contains a large amount of smectite, while Mix-2 contains a very small amount of smectite. Mix-1 has a higher Si abundance and lower Al and Fe abundances compared to Mix-2, and Mix-1 also has a greater LOI value which is consistent with smectites in this sample retaining more water than in Mix-2. Mix-1 has brighter reflectance in the visible/near-IR region and stronger ferric and phyllosilicate absorption bands, while Mix-2 has a more broad and rounded water band near 2.9-3.1 μm. In the mid-IR region Mix-1 exhibits more spectral contrast than Mix-2.

5. Results – Influence of Wet/Dry Cycling on Sample Texture and Spectroscopic Properties

Hydration/dehydration experiments were performed in order to test the effect of compositional differences on the formation of cemented crusts and to examine the effects of the resulting textures on the spectral properties of these cemented crusts. Images of the samples taken during this experiment are shown in Plate 1. The pair of smectite-bearing samples (soil Mix-1 and the iron oxyhydroxide-montmorillonite aggregate sample, "Fe-mont") exhibited swelling and cracking through the hydration/dehydration process as expected for smectites. Little difference was observed due to the addition of a sulfate component for this sample pair. For the palagonitic soil samples the presence of sulfates produced changes in the sample behavior as a function of hydration and dehydration. The palagonitic soil sample (Hal. Soil) showed a small amount of cracking and bubble formation, while the palagonitic soil plus sulfates mixture exhibited additional cracking and bubbling, as well as separation of some of the sulfate material from the sample mixture. The dehydration/rehydration cycling of sulfate-bearing soils appears to induce migration of the sulfate components to the surface. This was observed in another study [*Cooper and Mustard*, 2001] where the samples were heated for 20 minutes at 150 °C in order to retain the sulfate within the cemented crusts. Comparison of the cemented crusts formed from these two different materials showed that a harder, thicker crust (throughout the ~4 mm sample depth) formed for the smectite-dominated material, while a thinner (upper ~1 mm of the sample) and more friable crust resulted for the palagonitic soil (low smectite) based material.

14

Reflectance spectra are shown of the soil Mix-1 and Mix-2 samples in Figures 6 and 7 for the visible/NIR and mid-IR regions. In each case spectra were measured (A) of the particulate samples of the fine-grained aggregates that passed through a <125 μm sieve prior to the hydration experiments, (B) of the cemented samples hardened into crusts following the hydration/dehydration experiments, and (C) of the ground crusted samples that were passed through a <125 μm sieve. The smectite-based sample, Mix-1, exhibited much larger differences in NIR brightness as a function of sample texture than the palagonitic soil-based sample, Mix-2. For both samples the spectrum of the initial powder is the brightest, the reground sample is darker and the crusted sample is the darkest. The NIR and mid-IR absorption bands are significantly enhanced in the spectrum of the crusted Mix-1 sample compared to the other textures. The influence of sample texture and the presence of sulfates in soils observed here compare well with the recent work by *Cooper and Mustard* [2001] that explores these parameters in detail. Anhydrous magnesium sulfate was used in that study and strong sulfate bands were observed in the palagonitic soil crusts containing as little as 12.5 wt.% $MgSO_4$. Weaker sulfate bands are observed in our study because the total sulfate abundance is less than this.

TES data of Mars include atmospheric and surface components. Three distinct surface types have been identified to date and are attributed to basalt, andesite and a gray hematite [*Bandfield et al.*, 2000; *Christensen et al.*, 2000a,b]. The Martian basaltic and andesitic components have bands near 900-1100 and 300-500 cm^{-1} that compare well with bands observed in laboratory spectra of basaltic and andesitic rocks [*Hamilton and Christensen*, 2000; *Hamilton et al.*, 2001]. The silicate bands observed in spectra of Mix-1 and Mix-2 in this study fall in the same region as the silicate bands in the Martian basaltic and andesitic components and would be difficult to identify in the 3-5 km TES spot size on Mars if present as crusts scattered on the surface between rocks. *Cooper and Mustard* [2001b] found that the sulfate band near 1150 cm^{-1} varies with both sulfate concentration and cementation in their lab experiments. They determined that cemented soil units would need to comprise at least 10% of the area of a pixel in order to be identified in TES data. Recent investigations by *Cooper and Mustard* [2001a] with TES data indicate that sulfate cemented crusts may be present on Mars in several medium albedo regions including Lunae Planum, Isidis, parts of Arabia and others. They argue against evaporation of large-scale bodies of water as the formation mechanism for the sulfate crusts because these units are not

found in topographic lows. Their study suggests that the sulfate crusts are widely distributed on the planet, which is consistent with our model presented here.

6. Results – Comparison with IMP Spectra of Martian Soils and Rocks

The bidirectional reflectance data were convolved to Pathfinder Multispectral data using the filter positions and band passes of *Smith et al.* [1997]. These re-sampled lab spectra of the initial particulate Mix-1 and Mix-2 samples and the ground, cemented crusts of Mix-1 and Mix-2 are shown in Figure 8. The ground cemented crust spectra for both the smectite-based Mix-1 and the palagonitic soil based Mix-2 are darker than their respective particulate spectra measured prior to hydration/dehydration exposure. This suggests that sample texture and the degree of binding of the individual aggregates in the dust/soil particles contributes to the spectral brightness in this region. The bright, dark and disturbed Mars soil spectra are each an average of multiple IMP point spectra from bright, dark and disturbed soil deposits reported by *Yingst et al.* [1999]. The spectral character and composition of soils near the MPF lander have been described in detail by *Bell et al.* [2000] and *Morris et al.* [2000]. The Fe and S ratio of Mix-2 fall very close to the correlation line for Pathfinder soils reported in Fig. 39 of *Morris et al.* [2000] and that of Mix-1 falls somewhat below the line.

Re-sampled lab spectra are also shown in Figure 8 for the two solfataric volcanic soils used as endmembers in the mixtures. The sulfate-bearing Haleakala soil (250) spectrum contains a strong band minimum near 0.86 μm due to hematite and is less consistent with the MPF soil spectra. The character of the sulfate-bearing Santorini soil (182) spectrum includes the stronger curvature (0.6-0.67-0.75 μm) of the disturbed soils shown in Fig. 9. *Bridges et al.* [2001] compared spectral ratios with Si, Fe, Cl and S abundance of MPF soils and found multiple trends that are best explained by homogeneity in the soil units. Comparison of trends in many elements with S for soils at the MPF and Viking sites [*McSween and Keil*, 2000; *Morris et al.*, 2000] shows variations in the soil chemistry at the MPF site and between the MPF and Viking sites. Chemical analyses of MPF [*Bell et al.*, 2000; *Foley et al.*, 2001] and Viking [*Clark et al.*, 1982] soils in other studies also suggest compositional differences between the two sites.

Re-sampled lab spectra of the Mix-1 and Mix-2 cemented crusts and ground crusts are shown in Figure 9 along with IMP spectra of rocks near the MPF lander (from *Barnouin-Jha et al.* [2000] and re-sampled lab spectra of a martian meteorite (from *Bishop et al.* [1998b,c]. "Black"

rock exhibits fairly typical spectral properties in this region for the MPF site, with a few brigher rocks similar to "Shark" [*Murchie et al.*, 2000]. Rocks such as "Maroon" and "Orange" exhibit unique spectral character that has been attributed to the presence of coatings [*Barnouin-Jha et al.*, 2000]. The spectra of martian meteorite ALH 84001 contain a strong band near 0.93 μm due to orthopyroxene [*Bishop et al. 1998b,c*]. This band is much weaker in spectra of the MPF rocks and may be shifted towards longer wavelengths, which would be more consistent with a high-Ca pyroxene [*McSween et al.* 1999].

The spectrum of a ground portion of martian meteorite ALH 84001 is brighter than the ALH 84001 chip spectra and has a strong band near 0.93 μm and relatively high reflectance near 0.45 μm. The spectral character of this particulate ALH 84001 sample near 0.45 and 0.93 μm are very unlike the martian soil spectra shown in Figure 8. Rocks such as "Black" and "Shark" may exhibit different spectral properties from martian meteorites because they are mineralogically dissimilar or the rocks on Mars may be altered. Pyroxene and other minerals in these rocks may be weathered or the rocks may all contain coatings. Differences between the rocks "Black" and "Shark" and the rocks "Maroon" and "Orange" suggest that rock coatings are responsible for brighter reflectance in this region (especially for "Maroon"), a steeper slope from ~0.5 to 0.7 μm and a stronger ~0.9 μm band (especially for "Orange").

Spectra of the Mix-1 and Mix-2 cemented crusts ("B" in Figure 9) are darker in this region than spectra of the respective ground crusts ("C" in Figure 9). A cemented rock coating formed from something similar to Mix-1, comprising 10-15 wt.% Fe_2O_3 as nanophase Fe^{3+} oxyhydroxide in a silicate-sulfate matrix, could be responsible for the spectral features observed for the rock "Orange". A cemented rock coating containing schwertmannite or jarosite would also be consistent with the spectral properties of the rock "Orange" [*Barnouin-Jha et al.*, 2000]. A cemented rock coating created from dust similar to Mix-2, comprising 15-20 wt.% $Fe_2O_3^*$ as both Fe^{2+} in poorly crystalline silicates or glass and nanophase Fe^{3+} oxyhydroxides in a silicate-sulfate matrix, could be responsible for the spectral features observed for the rock "Maroon". Experiments involving abrasion of rock coatings by *Kraft and Greeley* [2000] found that varnishes composed of amorphous silica are resistant to abrasion and if present at the MPF site would be protecting the rocks. They further noted that dust aggregate particles would be ineffective abrasive agents at the MPF site. The results of *Kraft and Greeley* [2000] support the

formation of rock varnishes on Mars in accordance with our model of dust aggregates containing ferric oxides and sulfates in a poorly crystalline silicate matrix.

These chemically hardened coatings covering portions of the MPF rock surface are expected to be a few to hundreds of microns thick as observed for desert varnish on Earth. Because the spectral properties of altered rocks are distinct from those of cemented soil and appear to contain components due to the rock and the coating [*McSween et al.,* 1999; *Morris et al.,* 2000; *Bridges et al.,* 2001] it is assumed that these rock coatings are not optically thick. *Fischer and Pieters* [1993] found that viewing geometry, as well as composition and thickness of dust coatings, influences the spectral properties of fine-grained particles on a rock surface. Spectra measured of a 225 µm thick ferric oxide particles on basalt at incidence and emergence angles of 30° and 0°, respectively, produced a negative slope in the NIR region, while the spectra measured under specular configurations exhibited a much smaller positive slope [*Fischer and Pieters*, 1993].

7. Results – Physical evidence in volcanic environments

Volcanic ash is observed on Hawaii and Iceland at great distances from the active volcanic centers and is frequently observed as drift and cemented soil deposits. Shown in Plate 2 are examples of the terrain observed in the volcanic regions. Plate 2 (A) is an image taken of a rocky plain in western Iceland in the Laugarvatn mountain range. Fine-grained dust covered most surfaces in this region and multiple, rocky outcrops and crusted soil deposits were also observed. Plate 2 (B) is an image of a cemented deposit of altered volcanic ash in the southwestern region of the island of Hawaii. The ash in this region ranged from orange to light brown to black. Shown in Plate 2 (B) is an orange-pigmented crusted deposit partially covered by dark ash. In this location the orange crusted material was fixed and the black ash was loosely covering the surface and transported occasionally in the wind. A portion of this crusted material was tapped with a plastic trowel. The crust broke with a small force and revealed loose light brown ash underneath as shown in Plate 2 (C).

Drift deposits on Mars near the MPF lander were described by *McSween et al.* [1999] and motion within drift deposits has been analyzed in more detail by *Metzger* [2000]. The image of Mars containing Barnacle Bill in the lower right corner shown in Plate 2 (D) is a super-resolution image provided by T. Parker similar to that used by *Metzger* [2000]. The super-resolution images are made by deconvolving individual image frames and co-registering the group of

images which enables improved resolution [*Parker*, 1998]. Directional drift deposits are clearly visible in this image. The material contained in these drift deposits is the fine-grained dust/soil particles transported by aeolian processes. Some of this drift material is blown up onto the upper portions of rocks and may be trapped in crevices or ventifacts where it is less free to be transported away by aeolian forces.

The cemented crusts shown in Plate 2 (A, B, C) are terrestrial examples of what may be happening to the undisturbed ash deposits on Mars. Hardened crusts formed in laboratory experiments using fine-grained silicate-sulfate components described here and reported by *Cooper and Mustard* [2001] may also explain the "duricrust" and "hardpan" soil units observed by the Viking and Pathfinder cameras [*Binder et al.*, 1977; *Greeley et al.*, 1992; *Smith et al.*, 1997]. Sulfate transport through the ash particles during diurnal moisture cycling on Mars may be responsible for formation of the cemented soil units. Sulfate efflorescence to the sample surface can be seen in Plate 1 for soil Mix-2 after slowly dehydrating the sample in air and then in a desiccator. The lighter-colored ring along the outer surface of this sample is due to a higher concentration of sulfates. This was not observed for faster dehydration at 150 °C [*Cooper and Mustard* 2001]. These observations suggest that a small amount of sulfate in dust/soil particles would become more concentrated at the sample surface through mild/slow moisture cycling. Therefore, the diurnal moisture cycling on Mars may force these sulfate components to sample surfaces where they would be more readily able to react with other particles. Recent results by *Zent et al.* [2001] evaluating the H_2O adsorption kinetics on smectites found that the equilibration timescale for water vapor in smectites is too slow under martian early morning conditions. Their results suggest that the moisture is being adsorbed by another soil component. Possibly sulfates or nanophase ferric oxyhydroxides can adsorb H_2O faster than smectites and could account for adsorption of the early morning moisture.

8. Model Summary

Observations from the Viking and MPF landers have shown that many of the rock surfaces have coatings/alteration rinds and that the particles suspended in the atmosphere have many properties similar to those of the cemented soil and drift. This model was designed to explain the chemical, magnetic and spectroscopic properties of the surface material on Mars and is based on

a combination of palagonitic and solfataric alteration processes associated with volcanism and may include sulfates and other salts from evaporite deposits. This model involves both physical interactions, such as aeolian winds and electrostatic charges on dry particles, and chemical interactions including reaction of the sulfate phases and salts with water provided either by the diurnal moisture variations over long time periods or by melting ice flows or other more speculative forms of water.

The idea presented here is that 1-3 μm diameter dust/soil particles on Mars contain fine-grained silicate particles, formed through palagonitization or other alteration processes, that are mixed via aeolian processes with reactive sulfate or oxyhydroxide phases, produced on Mars via sofataric or evaporitic processes. The products formed through these processes are not required to be located near palagonitically altered volcanic material. The dust storms on Mars are continually transporting mobile fines across the surface and creating dunes and would, according to this model, actively mix nanophase to micron-sized particles across vast regions of the surface of Mars. Over time these dust particles become somewhat homogenized, although it is assumed that there would be regional differences. This dust is then transported and converted into the drift and cemented soil units observed on the surface, as well as rock coatings and varnishes on horizontal rock surfaces. The corrosive agents in the dust particles react over time forming the cemented soils/crusts and rock varnishes. These processes would also modify the chemistry and mineralogy of the surface crusts and rock alteration rinds as some elements are leached out of the silicate matrices and less resistant minerals are altered.

Cemented crusts in this study were formed using a mixture of silicates, sulfates and nanophase oxyhydroxides that is dominated by smectites and another that is dominated by palagonitically altered volcanic soil. The smectite-based Mix-1 exhibited significantly greater changes in both its binding properties throughout the hydration/dehydration cycling experiments and in its spectral properties following grinding of the hardened crust than did the palagonitic soil-based Mix-2. The hydration/dehydration experiments showed that a smectite component is not required for cementation of potential Mars analog soils into crusted material. The less reactive palagonitic soil Mix-2 allowed transport of water and sulfate to the surface forming a thin crust at the upper ~1 mm of the sample, while the more reactive smectite soil Mix-1 formed a cemented crust throughout the ~4 mm sample depth. The high smectite crust was also much harder than the low smectite crust. Future experiments on cemented soils are required in order to

better characterize the influence of specific silicate and sulfate minerals on crust formation mechanisms.

References

Adams, J.B., M.O. Smith, and P.E. Johnson, Spectral mixture modeling: A new analysis of rock and soil types at the Viking lander 1 site, *J. Geophys. Res.*, *91*, 8098-8112, 1986.

Arvidson, R.E., G.J. L., and H.J. Moore, The Martian surface as imaged, sampled, and analyzed by the Viking landers, *Rev. Geophys.*, *27*, 39-60, 1989.

Baker, V.R., R.G. Strom, V.C. Gulick, J.S. Kargel, G. Komatsu, and V.S. Kale, Ancient oceans, ice sheets and the hydrological cycle on Mars, *Nature*, *352*, 589-594, 1991.

Bandfield, J.L., V.E. Hamilton, and P.R. Christensen, A global view of martian surface compositions from MGS-TES, *Science*, *287*, 1626-1630, 2000.

Banin, A., F.X. Han, I. Kan, and A. Cicelsky, Acidic volatiles and the Mars soil, *J. Geophys. Res.*, *102*, 13,341-13,356, 1997.

Barnouin-Jha, O., S. Murchie, J. Johnson, J.F. Bell III, and R.V. Morris, Rock Coatings at the Mars Pathfinder Landing Site., in *Lunar Planet. Sci. XXXI.*, pp. CD-ROM #1267 (abstr.), Lunar Planet. Inst., Houston., 2000.

Bates, R.L., and J.A. Jackson, Dictionary of Geological Terms, pp. 571, Doubleday, New York, 1984.

Bell III, J.F., Iron, sulfate, carbonate, and hydrated minerals on Mars, in *Mineral Spectroscopy: A tribute to Roger G. Burns*, edited by M.D. Dyar, McCammon C., and M.W. Schaefer, pp. 359-380, The Geochemical Society, 1996.

Bell III, J.F., T.B. McCord, and P.D. Owensby, Observational evidence of crystalline iron oxides on Mars, *J. Geophys. Res.*, *95*, 14,447-14,461, 1990.

Bell III, J.F., H.Y. McSween Jr., S.L. Murchie, J.R. Johnson, R. Reid, R.V. Morris, R.C. Anderson, J.L. Bishop, N.T. Bridges, D.T. Britt, J.A. Crisp, T. Economou, A. Ghosh, J.P. Greenwood, H.P. Gunnlaugsson, R.M. Hargraves, S. Hviid, J.M. Knudsen, M.B. Madsen, H.J. Moore, R. Rieder, and L. Soderblom, Mineralogic and Compositional Properties of Martian Soil and Dust: Results from Mars Pathfinder, *J. Geophys. Res.*, *105*, 1721-1755, 2000.

Binder, A.B., R.E. Arvidson, E.A. Guinness, K.L. Jones, E.C. Morris, T.A. Mutch, D.C. Pieri, and C. Sagan, The geology of the Viking 1 Lander site, *J. Geophys. Res.*, *82*, 4439-4451, 1977.

Bishop, J., S. Murchie, C. Pieters, and A. Zent, A model for generation of martian surface dust, soil and rock coatings: Physical vs. Chemical interactions, and palagonitic plus hydrothermal alteration, in *5th Int'l Mars Conference*, pp. CD-ROM #6220 (abstr.), JPL, Pasadena, CA, 1999.

Bishop, J.L., and E. Murad, Schwertmannite on Mars? Spectroscopic analyses of schwertmannite, its relationship to other ferric minerals, and its possible presence in the surface material on Mars, in *Mineral Spectroscopy: A tribute to Roger G. Burns*, edited by M.D. Dyar, C.A. McCammon, and M.W. Schaefer, pp. 337-358, The Geochemical Society, 1996.

Bishop, J.L., and P. Smith, Results from Mars Pathfinder: Mineralogical composition of Martian dust and soils and a link to possible alteration processes on the Martian rocks, in *International Symposium on the Mars Exploration Programme and Sample Return Missions*, pp. abs. #O4/S2(182), ESA/CNES, Paris, France, 1999.

Bishop, J.L., H. Fröschl, and R.L. Mancinelli, Alteration processes in volcanic soils and identification of exobiologically important weathering products on Mars using remote sensing, *J. Geophys. Res.*, *103*, 31,457-31,476, 1998a.

Bishop, J.L., P. Schiffman, and R.J. Southard, Geochemical and mineralogical analyses of palagonitic tuffs and altered rinds of pillow lavas on Iceland and applications to Mars, *The Geological Society of London*, in press, 2001.

Bishop, J.L., C.M. Pieters, T. Hiroi, and J.F. Mustard, Spectroscopic analysis of martian meteorite ALH 84001 powder and applications for spectral identification of minerals and other soil components on Mars, *Meteorit. Planet. Sci.*, *33*, 699-708, 1998b.

Bishop, J.L., J.F. Mustard, C.M. Pieters, and T. Hiroi, Recognition of minor constituents in reflectance spectra of ALH 84001 chips and the importance for remote sensing on Mars, *Meteorit. Planet. Sci.*, *33*, 693-698, 1998c.

Bishop, J.L., C.M. Pieters, R.G. Burns, J.O. Edwards, R.L. Mancinelli, and H. Froeschl, Reflectance spectroscopy of ferric sulfate-bearing montmorillonites as Mars soil analog materials, *Icarus*, *117*, 101-119, 1995.

Bishop, J.L., A. Scheinost, J. Bell, D. Britt, J. Johnson, and S. Murchie, Ferrihydrite-schwertmannite-silicate mixtures as a model of Martian soils measured by Pathfinder, in *Lunar Planet. Sci. XXIX.*, pp. CD-ROM #1803 (abstr.), Lunar Planet. Inst., Houston., 1998d.

Bridges, N.T., J.A. Crisp, and J.F. Bell III, Characteristics of the Pathfinder APXS sites: Implications for the composition of Martian rocks and soils, *J. Geophys. Res.*, *106*, 14621-14665, 2001.

Bridges, N.T., R. Greeley, A.F.C. Haldemann, K.E. Herkenhoff, M. Kraft, T.J. Parker, and A.W. Ward, Ventifacts at the Pathfinder landing site, *J. Geophys. Res.*, *104*, 8595-8615, 1999.

Brückner, J., G. Dreibus, G.W. Lugmair, R. Rieder, H. Wänke, and T. Economou, Chemical composition of the Martian surface as derived from Pathfinder, Viking, and Martian meteorite data, in *Lunar Planet. Sci. XXX.*, pp. CDROM #1250 (abstr.), Lunar Planet. Inst., Houston., 1999.

Calvin, W.M., J.L. Bishop, and S. Erard, Clues from the SWIR: Mineralogical constraints from 1 to 4 µm, in *5th Mars Conference*, pp. CD-ROM #6125 (abstr.), JPL, Pasadena, CA, 1999.

Carr, M.H., *The Surface of Mars*, 232 pp., Yale Univ. Press, New Haven, 1981.

Christensen, P.R., J.L. Bandfield, and R.N. Clark, Edgett, K. S., Hamilton, V. E., Hoefen, T., Kieffer, H. H., Kuzmin, R. O., Lane, M. D., Malin, M. C., Morris, R. V., Pearl, J. C.,

Pearson, R., Roush, T. L., Ruff, S. W., Smith, M. D., Detection of crystalline hematite mineralization on Mars by the Thermal Emission Spectrometer: Evidence for near-surface water., *J. Geophys. Res.*, *105*, 9623-9642, 2000a.

Christensen, P.R., J.L. Bandfield, M.D. Smith, V.E. Hamilton, and R.N. Clark, Identification of basaltic component on the Martian surface from Thermal Emission Spectrometer Data, *J. Geophys. Res.*, *105*, 9609-9621, 2000b.

Clark, B.C., A.K. Baird, R.J. Weldon, D.M. Tsusaki, L. Schnabel, and M.P. Candelaria, Chemical composition of Martian fines, *J. Geophys. Res.*, *87*, 10059-10067, 1982.

Clifford, S.M., A model for the hydrological and climatic behavior of water on Mars, *J. Geophys. Res.*, *98*, 10,973-11,016, 1993.

Colman, S.M., Chemical weathering of basalts and andesites: Evidence from weathering rinds, US Geolog. Survey #1246, 1982.

Cooper, C.D., and J. Mustard, TES observations of the global distribution of sulfate on Mars, in *Lunar Planet. Sci. XXXII.*, pp. CD-ROM #2048 (abstr.), Lunar Planet. Inst., Houston., 2001a.

Cooper, C.D., and J.F. Mustard, Spectroscopy of loose and cemented sulfate-bearing soils: Implications for duricrust on Mars, *Icarus*, submitted, 2001b.

Crisp, J., and M.J. Bartholomew, Mid-infrared spectroscopy of Pahala ash palagonite and implications for remote sensing studies of Mars, *J. Geophys. Res.*, *97*, 14,691-14,699, 1992.

Dreibus, G., I. Ryabchikov, R. Rieder, T. Economou, J. Brückner, H.Y. McSween Jr., and H. Wänke, Relationship between rocks and soil at the Pathfinder landing site and the Martian meteorites, in *Lunar Planet. Sci. XXIX.*, pp. CDROM #1348 (abstr.), Lunar Planet. Inst., Houston., 1998.

Edgett, K.S., and M.C. Malin, Martian dust raising and surface albedo controls: Thin, dark (and sometimes bright) streaks and dust devils in MGS MOC high resolution images, in *Lunar Planet. Sci. XXXI.*, pp. CD-ROM #1073 (abstr.), Lunar Planet. Inst., Houston., 2000.

Farmer, C.B., D.W. Davies, A.L. Holland, D.D. LaPorte, and P.E. Doms, Mars: Water vapor observations from the Viking orbiters, *J. Geophys. Res.*, *82*, 4225-4248, 1977.

Fischer, E., and C.M. Pieters, The continuum slope of Mars: Bi-directional reflectance investigations and applications to Olympus Mons, *Icarus*, *102*, 185-202, 1993.

Fisher, R.V., and H.-U. Schminke, *Pyroclastic rocks*, 742 pp., Springer-Verlag, New York, 1984.

Foley, C.N., T.E. Economou, and R.N. Clayton, Chemistry of Mars Pathfinder samples determined by the APXS, in *Lunar Planet. Sci. XXXII.*, pp. CD-ROM #1979 (abstr.), Lunar Planet. Inst., Houston., 2001.

Golombek, M.P., R.A. Cook, H.J. Moore, and T.J. Parker, Selection of the Mars Pathfinder landing site, *J. Geophys. Res.*, *102*, 3967-3988, 1997.

Greeley, R., N. Lancaster, S. Lee, and P. Thomas, Martian aeolian processes, sediments, and features, in *Mars*, edited by H.H. Kieffer, B.M. Jakosky, C.W. Snyder, and M.S. Matthews, pp. 730-766, Univ. Arizona Press, Tucson, 1992.

Greeley, R., M. Kraft, R. Sullivan, G. Wilson, N. Bridges, K. Herkenhoff, R.O. Kuzmin, M. Malin, and W. Ward, Aeolian features and processes at the Mars Pathfinder landing site, *J. Geophys. Res.*, *104*, 8573-8584, 1999.

Guinness, E.A., R.E. Arvidson, I.H.D. Clark, and M.K. Shepard, Optical scattering properties of terrestrial varnished basalts compared with rocks and soils at the Viking Lander sites, *J. Geophys. Res., 102*, 28687-28703, 1987.

Hamilton, V.E., and P.R. Christensen, Determining the modal mineralogy of mafic and ultramafic igneous rocks using thermal emission spectroscopy, *J. Geophys. Res., 105*, 9701-9716, 2000.

Hamilton, V.E., M.B. Wyatt, H.Y. McSween Jr., and P.R. Christensen, Analysis of terrestrial and Martian volcanic compositions using thermal emission spectroscopy: 2. Application to Martian surface spectra from the Mars Global Surveyor Thermal Emission Spectrometer, *J. Geophys. Res., 106*, 14,733-14,746, 2001.

Hargraves, R.B., D.W. Collinson, R.E. Arvidson, and C.R. Spitzer, The Viking magnetic properties experiment: Primary mission results., *J. Geophys. Res., 82*, 4547-4558, 1977.

Hoffman, N., White Mars: A new model for Mars' surface and atmosphere based on CO_2, *Icarus, 146*, 326-342, 2000.

Hviid, S.F., M.B. Madsen, H.P. Gunnlaugsson, W. Goetz, J.M. Knudsen, R.B. Hargraves, P. Smith, D. Britt, A.R. Dinesen, C.T. Mogensen, M. Olsen, C.T. Pedersen, and L. Vistisen, Magnetic Properties Experiments on the Mars Pathfinder Lander: Preliminary Results, *Science, 278*, 1768-1771, 1997.

Johnson, J.R., Thermal infrared reflectance and emission spectra of Mars-like dust coatings on basalt substrates, in *Lunar Planet. Sci. XXX*, pp. CD-ROM #1214 (abstr.), Lunar Planet. Inst., Houston., 1999.

Kraft, M.D., and R. Greeley, Rock coatings and aeolian abrasian on Mars: Application to the Pathfinder landing site, *J. Geophys. Res., 105*, 15,107-15,116, 2000.

Madsen, M.B., S.F. Hviid, H.P. Gunnlaugsson, J.M. Knudsen, W. Goetz, C.T. Pedersen, A.R. Dinesen, C.T. Mogensen, and M. Olsen, The magnetic properties experiment on Mars Pathfinder, *J. Geophys. Res., 104*, 8761-8779, 1999.

Malin, M., and K.S. Edgett, Sedimentary rocks of early Mars, *Science, 290*, 1927-1937, 2000a.

Malin, M.C., and K.S. Edgett, Evidence for recent groundwater seepage and surface runoff on Mars, *Science, 288*, 2330-2335, 2000b.

McLennan, S.M., Chemical composition of Martian soil and rocks: Complex mixing and sedimentary transport, *Geophys. Res. Lett., 27*, 1335-1338, 2000.

McSween Jr., H.Y., and K. Keil, Mixing relationships in the Martian regolith and the composition of the globally homogeneous dust, *Geochim. Cosmochim. Acta, 64*, 2155-2166, 2000.

McSween Jr., H.Y., S.L. Murchie, J.A. Crisp, N.T. Bridges, R.C. Anderson, J.F. Bell III, D.T. Britt, J. Brückner, G. Dreibus, T. Economou, A. Ghosh, M.P. Golombek, J.P. Greenwood, J.R. Johnson, H.J. Moore, R.V. Morris, T.J. Parker, R. Rieder, R. Singer, and H. Wänke, Chemical, multispectral, and textural constraints on the composition and origin of rocks at the Mars Pathfinder landing site, *J. Geophys. Res., 104*, 8679-8715, 1999.

Metzger, S.M., Shifting wind regines at MPF as evidenced by wind tail bedding, in *Lunar Planet. Sci. XXXI.*, pp. CD-ROM #2095 (abstr.), Lunar Planet. Inst., Houston., 2000.

Metzger, S.M., J.R. Carr, J.R. Johnson, T.J. Parker, and M. Lemmon, Dust devil vortices seen by the Mars Pathfinder camera, *Geophys. Res. Lett., 26*, 2781-2784, 1999.

Minitti, M.E., M.J. Rutherford, and J.F. Mustard, The effects of oxidation on spectra of SNC-like basalts: Applications to Mars remote sensing, in *Lunar Planet. Sci. XXXI.*, pp. CD-ROM #1282 (abstr.), Lunar Planet. Inst., Houston., 2000.

Morris, R.V., D.C. Golden, and J.F. Bell III, Low-temperature reflectivity spectra of red hematite and the color of Mars, *J. Geophys. Res., 102*, 9125-9133, 1997.

Morris, R.V., D.C. Golden, J.F. Bell III, and H.V. Lauer Jr., Hematite, pyroxene, and phyllosilicates on Mars: Implications from oxidized impact melt rocks from Manicouagan Crater, Quebec, Canada, *J. Geophys. Res., 100*, 5319-5328, 1995.

Morris, R.V., D.W. Ming, D.C. Golden, and J.F. Bell III, An occurrence of jarosite tephra on Mauna Kea, Hawaii: Implications for the ferric mineralogy of the Martian surface, in *Mineral Spectroscopy: A tribute to Roger G. Burns*, edited by M.D. Dyar, C. McCammon, and M.W. Schaefer, pp. 327-336, The Geochemical Society, 1996.

Morris, R.V., D.C. Golden, T.D. Shelfer, and H.V. Lauer Jr., Lepidocrocite to maghemite to hematite: A pathway to magnetic and hematitic Martian soil, *Meteorit. Planet. Sci., 33*, 743-751, 1998.

Morris, R.V., D.C. Golden, J.F. Bell III, H.V. Lauer Jr., and J.B. Adams, Pigmenting agents in Martian soils: Inferences from spectral, Mössbauer, and magnetic properties of nanophase and other iron oxides in Hawaiian palagonitic soil PN-9, *Geochim. Cosmochim. Acta, 57*, 4597-4609, 1993.

Morris, R.V., D.C. Golden, D.W. Ming, T.D. Shelfer, L.C. Jørgensen, J.F. Bell III, T.G. Graff, and S.A. Mertzman, Phyllosilicate-poor palagonitic dust from Mauna Kea volcano (Hawaii): A mineralogical analogue for magnetic Martian dust?, *J. Geophys. Res., 106*, 5057-5083, 2001.

Morris, R.V., D.C. Golden, J.F. Bell III, T.D. Shelfer, A.C. Scheinost, N.W. Hinman, G. Furniss, S.A. Mertzman, J.L. Bishop, D.W. Ming, C.C. Allen, and D.T. Britt, Mineralogy, composition, and alteration of Mars Pathfinder rocks and soils: Evidence from multispectral, elemental, and magnetic data on terrestrial analogue, SNC meteorite, and Pathfinder samples, *J. Geophys. Res., 105*, 1757-1817, 2000.

Murchie, S., O. Barnouin-Jha, J. Johnson, J.F. Bell III, H.Y. McSween Jr., and R.V. Morris, Diverse Rock Types at the Mars Pathfinder Landing Site., in *Lunar Planet. Sci. XXXI.*, pp. CD-ROM #1267 (abstr.), Lunar Planet. Inst., Houston., 2000.

Musselwhite, D.S., T.D. Swindle, and J.I. Lunine, Liquid CO_2 breakout and the formation of recent small gullies on Mars, in *Lunar Planet. Sci. XXXII.*, pp. CD-ROM #1030 (abstr.), Lunar Planet. Inst., Houston., 2001.

Nesbitt, H.W., and G.M. Young, Prediction of some weathering trends of plutonic and volcanic rocks based on thermodynamic and kinetic considerations, *Geochim. Cosmochim. Acta, 48*, 1523-1534, 1984.

Newsom, H.E., J.J. Hagerty, and F. Goff, Mixed hydrothermal fluids and the origin of the Martian soil, *J. Geophys. Res., 104*, 8717-8728, 1999.

Parker, T.J., "Super resolution" of the Mars Pathfinder landing site, using manual techniques, in *Lunar Planet. Sci. XXIX.*, pp. CD-ROM #1817 (abstr.), Lunar Planet. Inst., Houston., 1998.

Parker, T.J., D.S. Gorsline, R.S. Saunders, D.C. Pieri, and D.M. Schneeberger, Coastal Geomorphology of the Martian Northern Plains, *J. Geophys. Res., 98*, 11061–11078, 1993.

Pieters, C.M., Strength of mineral absorption features in the transmitted component of near-infrared reflected light: First results from RELAB, *J. Geophys. Res.*, *88*, 9534-9544, 1983.

Pollack, J.B., M.E. Ockert-Bell, and M.K. Shepard, Viking lander image anaylsis of Martian atmospheric dust, *J. Geophys. Res.*, *100*, 5235-5250, 1995.

Pollack, J.B., D. Colburn, R. Kahn, J. Hunter, W. VanCamp, and B. Baldwin, Properties of aerosols in the Martian atmosphere, as inferred from Viking lander data, *J. Geophys. Res.*, *82*, 4479-4496, 1977.

Pollack, J.B., D.S. Colburn, F.M. Flasar, R. Kahn, C.E. Carlston, and D. Pidek, Properties and effects of dust particles suspended in the Martian atmosphere, *J. Geophys. Res.*, *84*, 2929-2945, 1979.

Roush, T.L., D.L. Blaney, and R.B. Singer, The surface composition of Mars as inferred from spectroscopic observations, in *Remote Geochemical Analysis: Elemental and Mineralogical Composition*, edited by C.M. Pieters, and P.A.J. Englert, pp. 367- 393, Cambridge University Press, Cambridge, 1993.

Ruff, S.W., and P.R. Christensen, Thermal-infrared spectral characteristics of Martian albedo features: Clues to composition, in *5th Int'l Mars Conference*, pp. CD-ROM #6230 (abstr.), JPL, Pasadena, CA, 1999.

Scheinost, A.C., A. Chavernas, V. Barrón, and J. Torrent, Use and limitations of second-derivative diffuse reflectance spectroscopy in the visible to near-infrared range to identify and quantify Fe oxide minerals in soils, *Clays Clay Miner.*, *46*, 528-536, 1998.

Schiffman, P., H.J. Spero, R.J. Southard, and D.A. Swanson, Controls on palagonitization versus pedogenic weathering of basaltic tephra: Evidence from the consolidation and geochemistry of the Keanakako'i ash member, Kilauea volcano, *Geochemistry Geophysics Geosystems*, *1*, Paper no. 2000GC000068, 2000.

Schiffman, P., R.J. Southard, D.D. Eberl, and J.L. Bishop, Distinguishing palagonitization from other forms of alteration of basaltic tephra: mineralogical and geochemical criteria, *The Geological Society of London*, in press, 2001.

Schultz, P.H., and J.F. Mustard, Martian impact glass: Generation and evidence, in *Lunar Planet. Sci. XXIX.*, pp. CD-ROM #1847 (abstr.), Lunar Planet. Inst., Houston., 1998.

Smith, P.H., and M. Lemmon, Opacity of the Martian atmosphere measured by the Imager for Mars Pathfinder, *J. Geophys. Res.*, *104*, 8975-8985, 1999.

Smith, P.H., J.F. Bell III, N.T. Bridges, D.T. Britt, L. Gaddis, R. Greeley, H.U. Keller, K.E. Herkenhoff, R. Jaumann, J.R. Johnson, R.L. Kirk, M. Lemmon, J.N. Maki, M.C. Malin, S.L. Murchie, J. Oberst, T.J. Parker, R.J. Reid, R. Sablotny, L.A. Soderblom, C. Stoker, R. Sullivan, N. Thomas, M.G. Tomasko, W. Ward, and E. Wegryn, Results from the Mars Pathfinder camera, *Science*, *278*, 1758-1765, 1997.

Soderblom, L.A., The composition and mineralogy of the Martian surface from spectroscopic observations: 0.3-50 μm, in *Mars*, edited by H.H. Kieffer, B.M. Jakosky, C.W. Snyder, and M.S. Matthews, pp. 557-593, Univ. of Arizona Press, Tucson, 1992.

Sprague, A.L., D.M. Hunten, R.E. Hill, B. Rizk, and W.K. Wells, Martian water vapor, 1988-1995, *J. Geophys. Res.*, *101*, 23,229-23,241, 1996.

Staudigel, H., and S.R. Hart, Alteration of basaltic glass: Mechanisms and significance for the oceanic crust-seawater budget, *Geochim. Cosmochim. Acta*, *47*, 337-350, 1983.

Thomas, N., W.J. Markiewicz, R.M. Sablotny, M.W. Wuttke, H.U. Keller, J.R. Johnson, R.J. Reid, and P.H. Smith, The color of the Martian sky and it sinfluence on the illumination of the Martian surface, *J. Geophys. Res., 104*, 8795-8808, 1999.

Thomas, P., and P.J. Gierasch, Dust devils on Mars, *Science, 230*, 175-177, 1985.

Titov, D.V., J. Rosenqvist, V.I. Moroz, A.V. Grigoriev, and G. Arnold, Evidences of the regolith-atmosphere water exchange on Mars from the ISM (Phobos-2) infrared spectrometer observations, *Adv. Space Research, 16 (6)*, 23-33, 1995.

Tomasko, M.G., L.R. Doose, M. Lemmon, P.H. Smith, and E. Wegryn, Properties of dust in the Martian atmosphere from the Imager on Mars Pathfinder, *J. Geophys. Res., 104*, 8987-9008, 1999.

Wänke, H., Results from APXS on Pathfinder, in *International Symposium on the Mars Exploration Programme and Sample Return Missions*, pp. abs. #O1/S2(131), ESA/CNES, Paris, France, 1999.

Yingst, R.A., R.J. Reid, and P.H. Smith, Preliminary science results from the recalibration of IMP images, in *5th Int'l Mars Conference*, pp. CD-ROM #6199 (abstr.), JPL, Pasadena, CA, 1999.

Zent, A.P., D.J. Howard, and R.C. Quinn, H_2O adsorption on smectites: Application to the diurnal variation of H_2O in the Martian atmosphere, *J. Geophys. Res., 106*, 14,667-14,674, 2001.

Plate Captions

Plate 1 Images of samples in wet/dry cycling experiments. Mix-1 is shown at the top, followed by the iron oxyhydroxide-montmorillonite aggregate sample that makes up a substantial portion of Mix-1. Mix-2 is shown next followed by the palagonitically altered Haleakala ash sample that makes up a substantial portion of Mix-2. The samples were (A) dried in a desiccator, (B) hydrated with H₂O, (C) dehydrated in the desiccator, and (D) dehydrated in the desiccator following a second hydration cycle.

Plate 2 Drift and cemented soil deposits from Iceland, Hawaii, and Mars. Shown in (A) is an image taken of a rocky plain in western Iceland in the Laugarvatn mountain range; fine-grained dust, rocky outcrops and crusted soil were observed in this region. The red bar indicates approximately 1 meter. Shown in (B) is an image of a cemented deposit of altered volcanic ash on the island of Hawaii and (C) is an enlarged version of the broken crust pieces from (B) following scraping of the surface with a plastic trowel. The red bar is ~1 meter long in (B) and ~10 cm long in (C) and the white box on (B) indicates the approximate region of image (C) prior to breaking the surface crust. The dark material is fine-grained (presumable less altered) volcanic ash. Shown in (D) is a super-resolution image of Barnacle Bill provided by T. Parker and modified after *Metzger* [2000].

Figure Captions

Fig. 1 Model of dust reactions. Dust particles are shown near the top of this diagram. These are distributed via aeolian processes and settle on top of rocks and between rocks on Mars forming drift deposits of dust/soil particles and physical layers of dust as rock coatings. Aeolian processes may redistribute these drift and rock coating deposits back into the atmosphere as dust particles or elsewhere on the surface. Chemical interaction of the dust/soil particles in the drift deposits forms a hardened, cemented soil that can no longer be freely redistributed by aeolian processes. Chemical interaction of the dust/soil particles deposited on rock surfaces forms a hardened rock varnish above a chemically leached layer of rock.

Fig. 2 Model of surface reactions. Possible chemical reactions occurring on the surfaces of dust/soil particles and rocks are shown here. Iron oxyhydroxide species and sulfate salts are examples of reactive components that could bind together chemically neutral silicate particles in the dust/soil particles.

Fig. 3 Model of aggregate particles. This diagram shows a physical mixture on the left of iron oxide/oxyhydroxide, sulfate and silicate grains as well as clay aggregate particles. These clay aggregate particles are examples of chemical mixtures. A chemical mixture of intergrown, nanophase-sized grains is shown on the right.

Fig. 4 Reflectance spectra from 0.3 to 5 µm of the new mixtures and their endmember s. Each mixture contains 10 wt.% each of hydrated magnesium sulfate (MgSO₄•7H₂O), and sulfate-bearing volcanic soils from Santorini and Haleakala. Mix-1 contains 70 wt.% of an iron oxyhydroxide-montmorillonite aggregate soil and Mix-2 contains 70 wt.% of palagonitically altered ash from Haleakala.

Fig. 5 Reflectance spectra from 400 to 2000 cm^{-1} (5 to 25 μm) of the new mixtures and their endmembers. The mixtures are as described in Fig. 4 and in the text.

Fig. 6 Reflectance spectra from 0.3 to 5 μm of two dust/soil analog mixtures (A) particulate samples of fine-grained aggregates passed through a <125 μm sieve, (B) cemented samples hardened into crusts by adding H$_2$O and drying, and (C) ground crusted samples that were passed through a <125 μm sieve.

Fig. 7 Reflectance spectra from 400 to 2000 cm^{-1} (5 to 25 μm) of two dust/soil analog mixtures (A) particulate samples of fine-grained aggregates passed through a <125 μm sieve, (B) cemented samples hardened into crusts by adding H$_2$O and drying, and (C) ground crusted samples that were passed through a <125 μm sieve.

Fig. 8 Extended visible region reflectance spectra of dust/soil analog mixtures in comparison with Martian soil spectra. Versions (A) and (C) of Mix-1 and Mix-2 are the fluffy and re-ground particulate samples as described in the text and Fig. 7. These data were convolved to Pathfinder multispectral data using the filter positions and band passes of *Smith et al.* [1997]. The bright, dark and disturbed soil spectra are averages of multiple IMP point spectra from bright, dark and disturbed soil deposits reported by *Yingst et al.* [1999].

Fig. 9 Extended visible region reflectance spectra of analog mixtures in comparison with Martian rock and meteorite spectra. Versions (B) and (C) of Mix-1 and Mix-2 are the cemented crusts and re-ground particulate samples as described in the text and Fig. 7. These data were convolved to IMP filter positions and band passes. The IMP spectra of martian rocks are from *Barnouin-Jha et al.* [2000] and the martian meteorite spectra are from *Bishop et al.* [1998b,c] .

Table 1. Chemical Composition of Mars Soil and Laboratory Samples

	Mars Soil MPF- ave	Mix-1 (364)	Mix-2 (365)	Fe-Mont (11)	Hal soil (248)	Sant soil (182)	Hal soil (250)	Mg-Sulfate (366)
SiO$_2$	40.6	43.7	28.0	54.3	31.9	33.3	23.2	0.0
TiO$_2$	0.9	0.4	3.8	0.1	5.0	1.3	2.1	0.0
Al$_2$O$_3$	9.6	13.9	19.3	16.2	23.9	15.0	10.4	0.0
Fe$_2$O$_3$*	22.3	13.6	18.7	12.0	19.3	9.1	43.2	0.0
MgO	8.3	3.1	3.1	1.9	1.9	0.1	1.1	16.4
CaO	5.8	0.5	4.0	0.1	5.2	0.4	3.4	0.0
Na$_2$O	3.5	1.3	0.8	1.6	0.8	1.0	1.1	0.0
K$_2$O	0.9	0.5	0.6	0.3	0.4	1.6	1.1	0.0
SO$_3$	6.1	4.9	5.0	0.0	0.2	10.8	5.8	32.5
LOI	n.d.	17.9	14.8	14.2	9.9	20.9	7.5	51.2
SUM	98.0	99.8	98.1	100.7	98.5	93.5	98.9	100.1

Mix-1(364): 70wt% (11) + 10wt% (182) + 10wt% (250) + 10wt% (366)

Mix-2 (365): 70wt% (248) + 10wt% (182) + 10wt% (250) + 10wt% (366)

Note: data are in wt.%, Fe is shown as Fe$_2$O$_3$* and includes FeO and Fe$_2$O$_3$, n.d. is not determined, LOI is lost on ignition at 850 °C, mixture chemistries are calculated from their components, Mars Pathfinder (MPF) soil average determined from data reported by *Foley et al.* [2001], iron oxyhydroxide-montmorillonite aggregate (Fe-mont) sample chemistry from *Bishop et al.* [1995], volcanic soil chemistries from *Bishop et al.* [1998a].

Figure 1

Model of Dust Reactions

dust particles

drift   rock coating

rock

cemented soil   rock varnish

rock
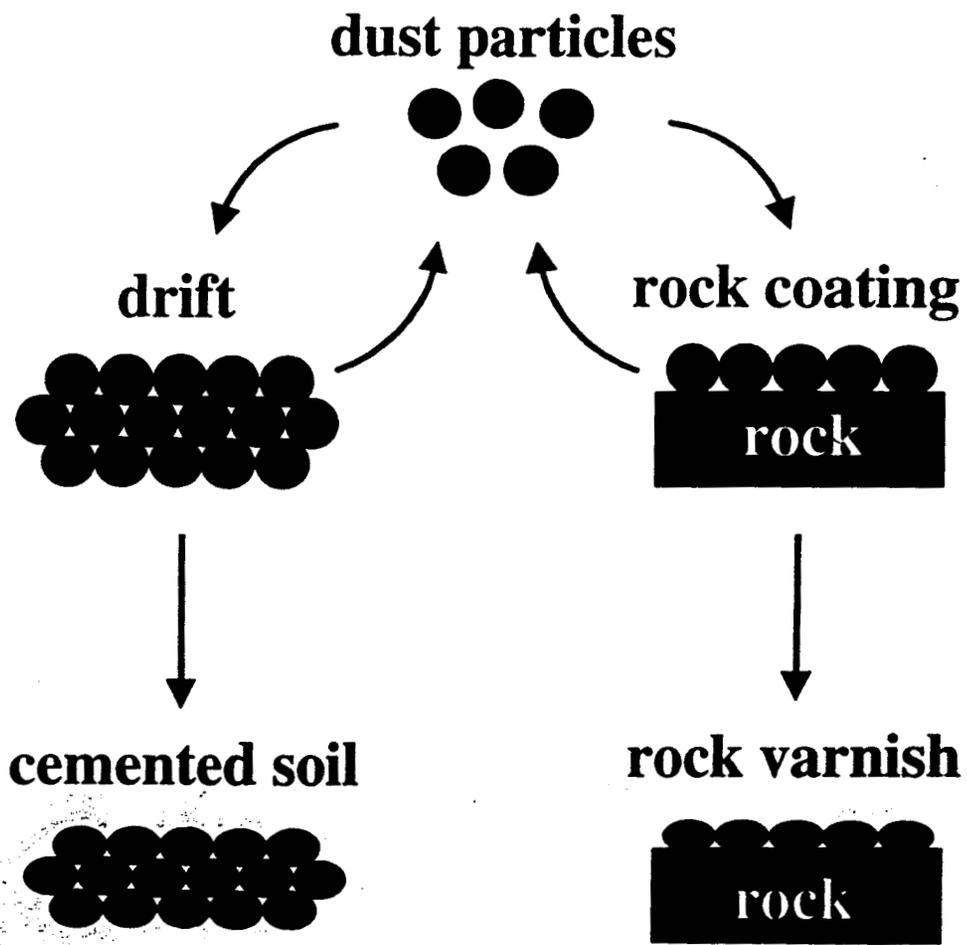
Figure 2

<u>Model of Surface Reactions</u>
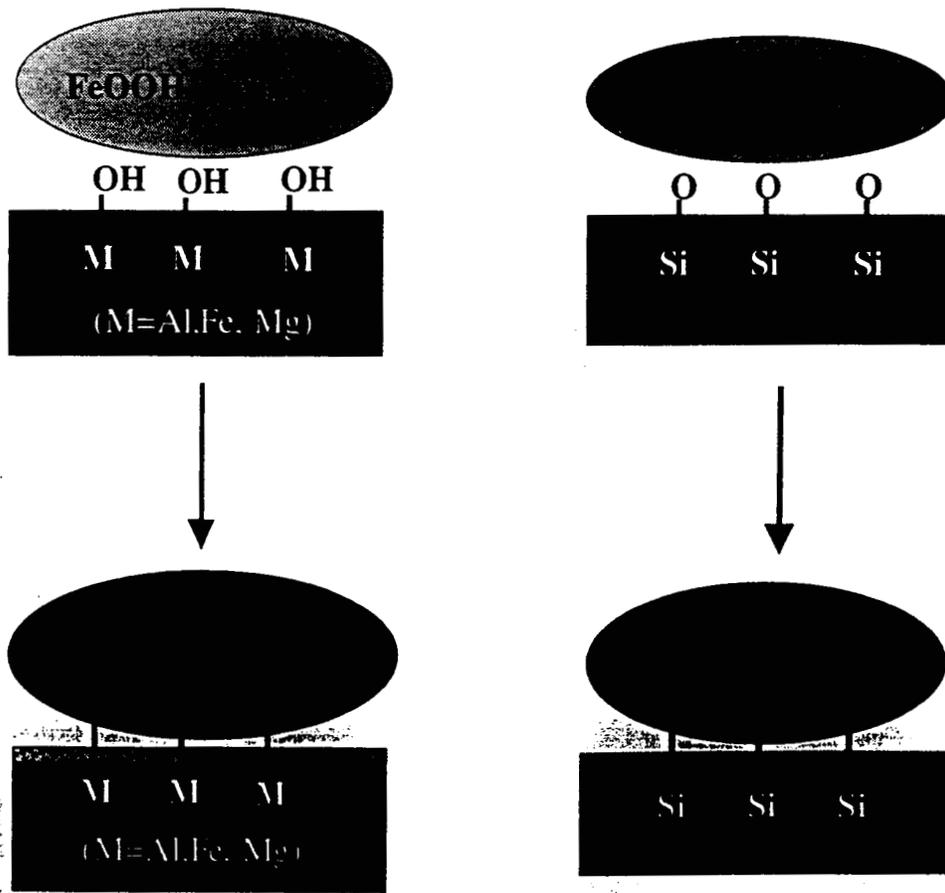
Figure 3

Model of Aggregate Particles in Dust

clay aggregates

~1 μm

Fe oxide grains →

sulfate grains →

silicate grains →

~10 μm
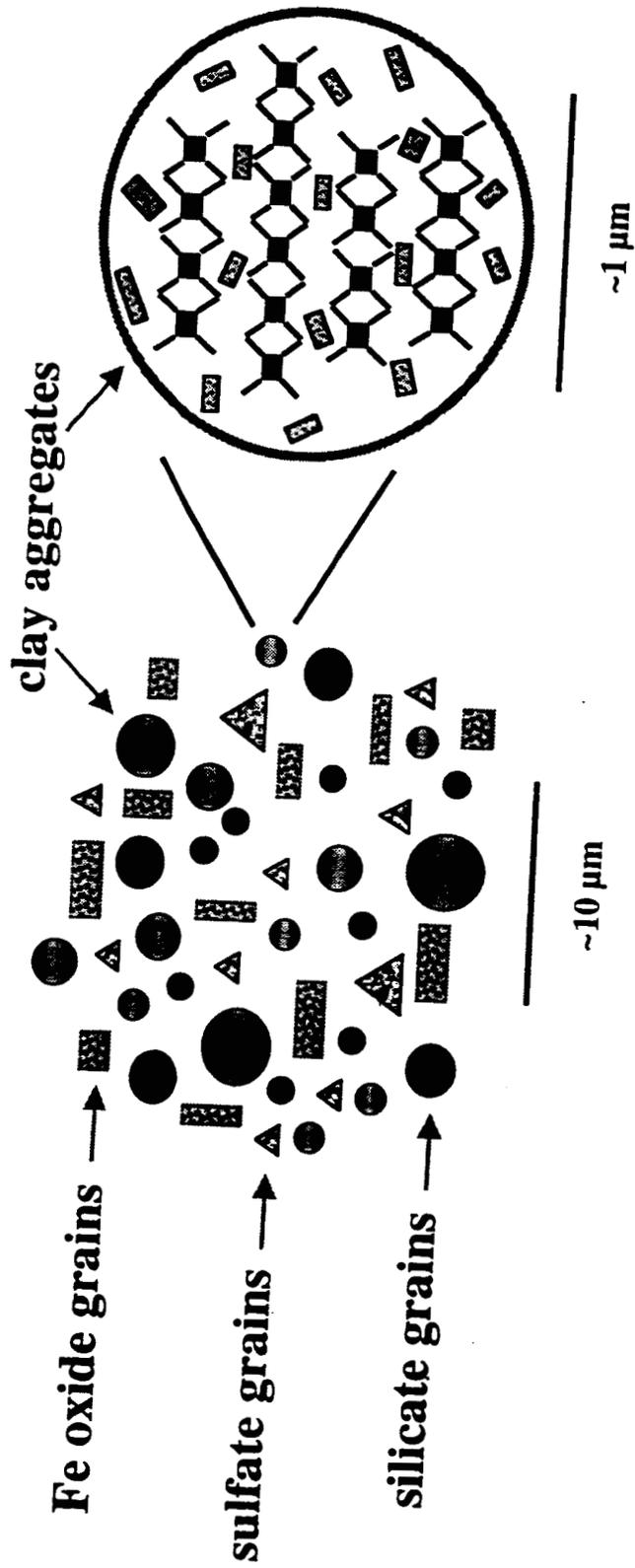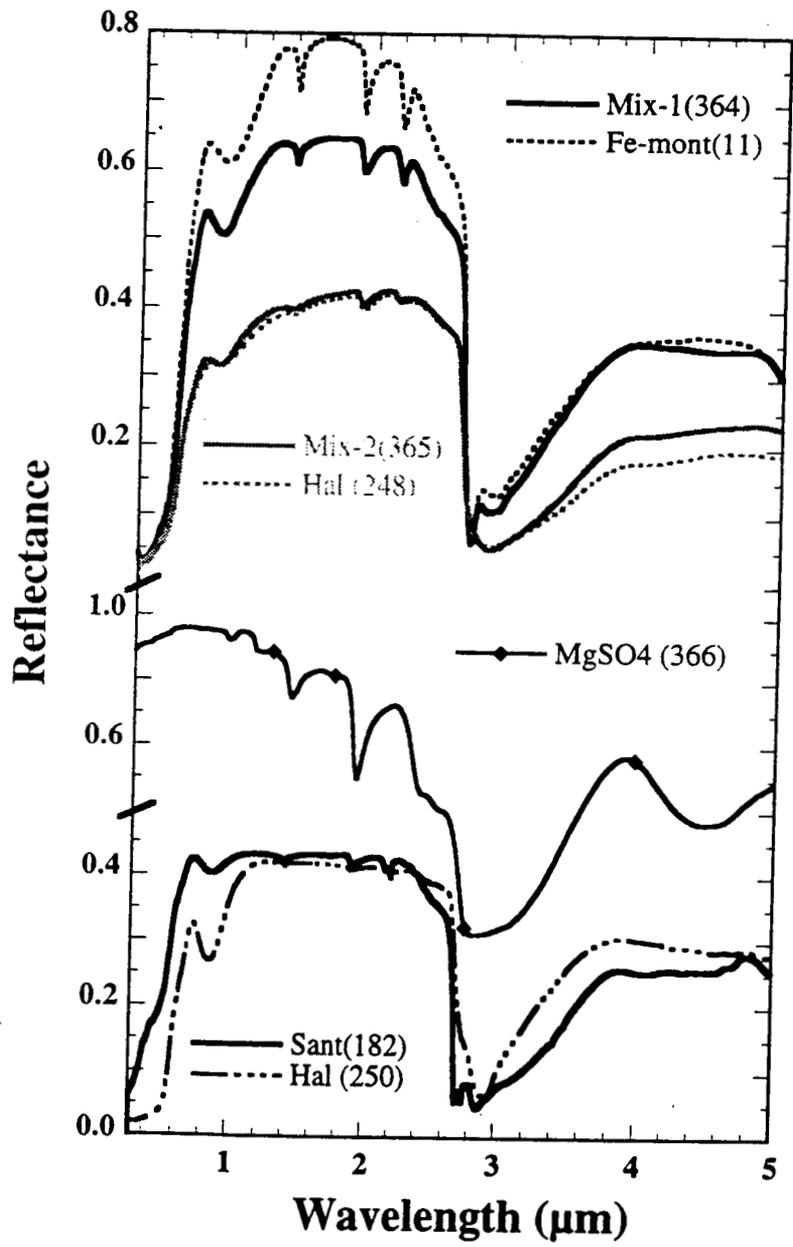
Figure 4

Figure 4

Figure 5

Figure 6

Figure 7

Reflectance vs Wavelength (µm)

Analog Soils
— Mix-1 (A)
— Mix-1 (C)

Martian Soils
---◇--- Sant. soil (182)
----△---- Hal. soil (250)
—○— Mix-2 (A)
—▲— Mix-2 (C)
Bright soil (ave)
Dark soil (ave)
Dist. soil (ave)

Reflectance vs Wavelength (µm)

Analog Soils
—▼— Mix-1 (C)
--△-- Mix-1 (B)
— Mix-2 (C)
--▲-- Mix-2 (B)

Martian Rocks
---△--- "Maroon"
—□— "Orange"
---●--- "Shark"
--▲-- "Black"

Martian Meteorite ALH 84001
split 271, chip
split 92, chip
split 92, <125 µm
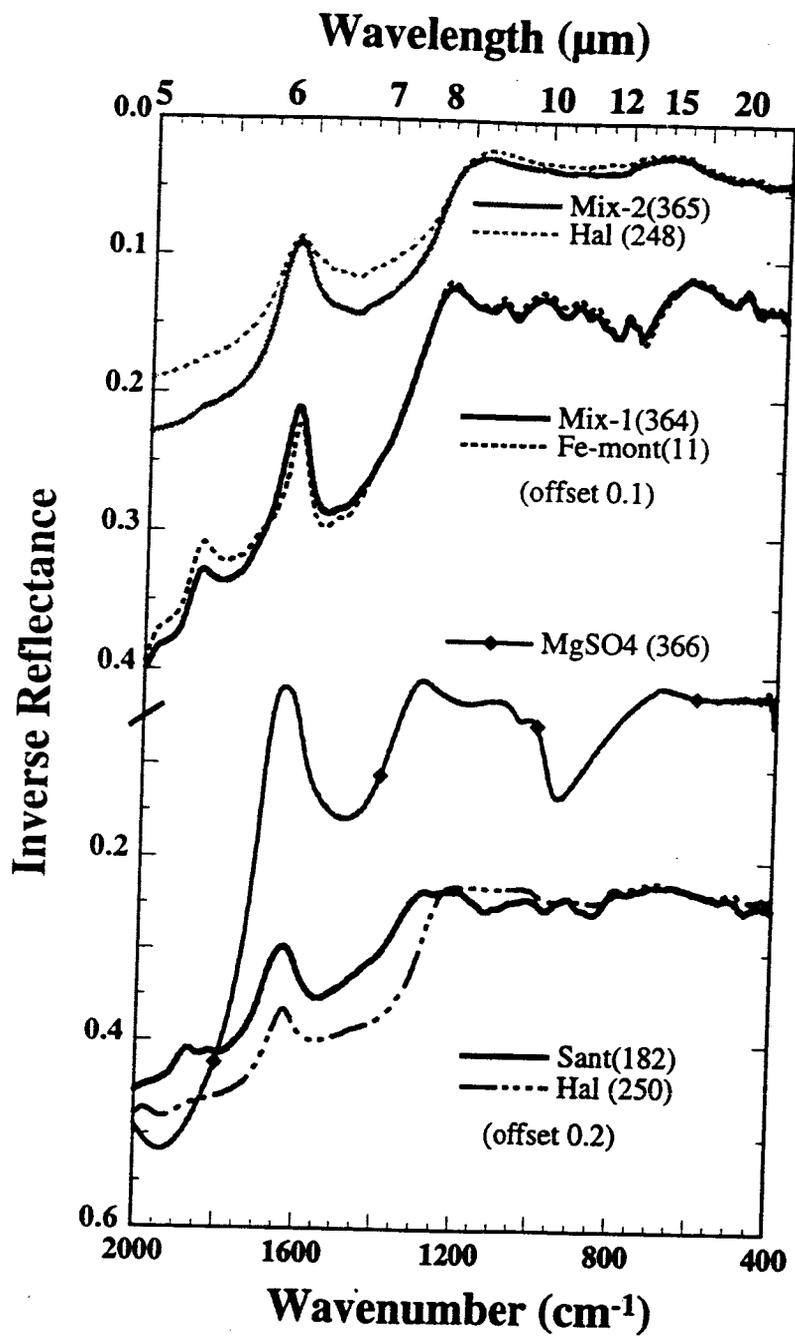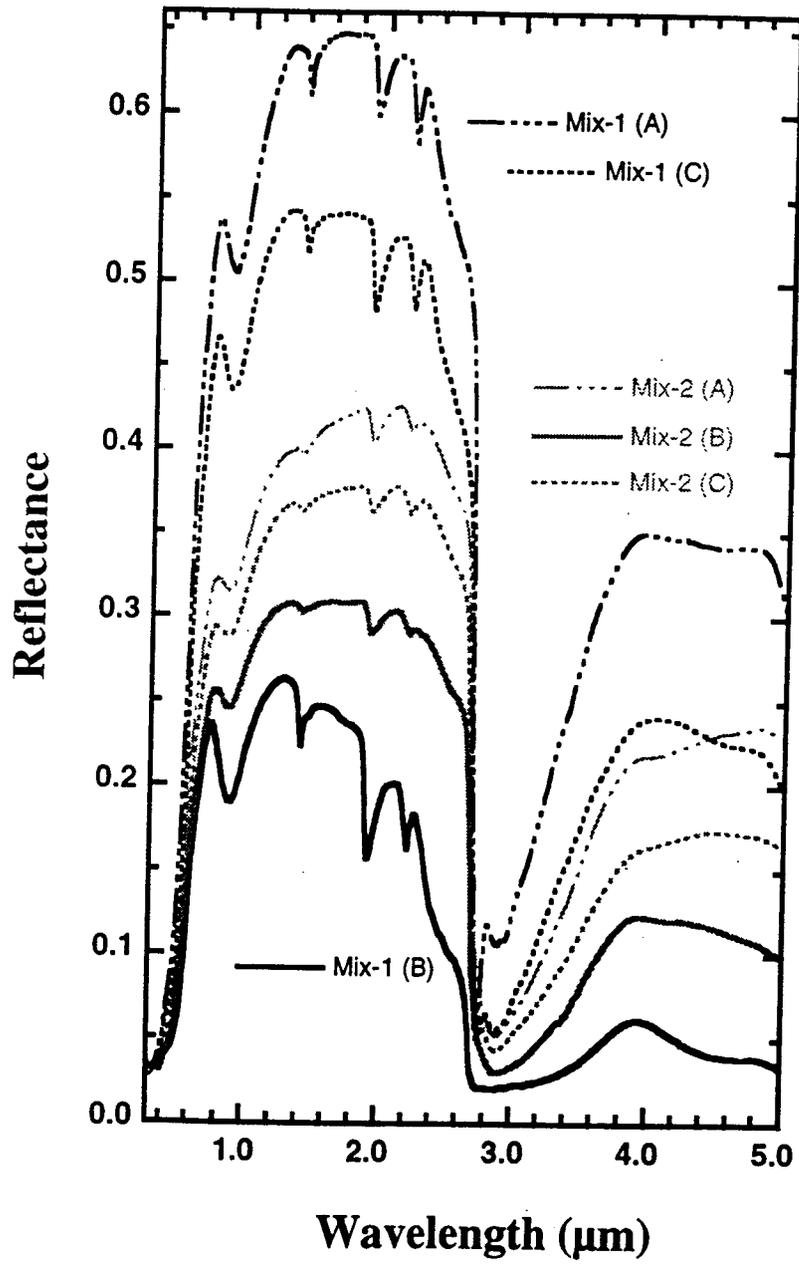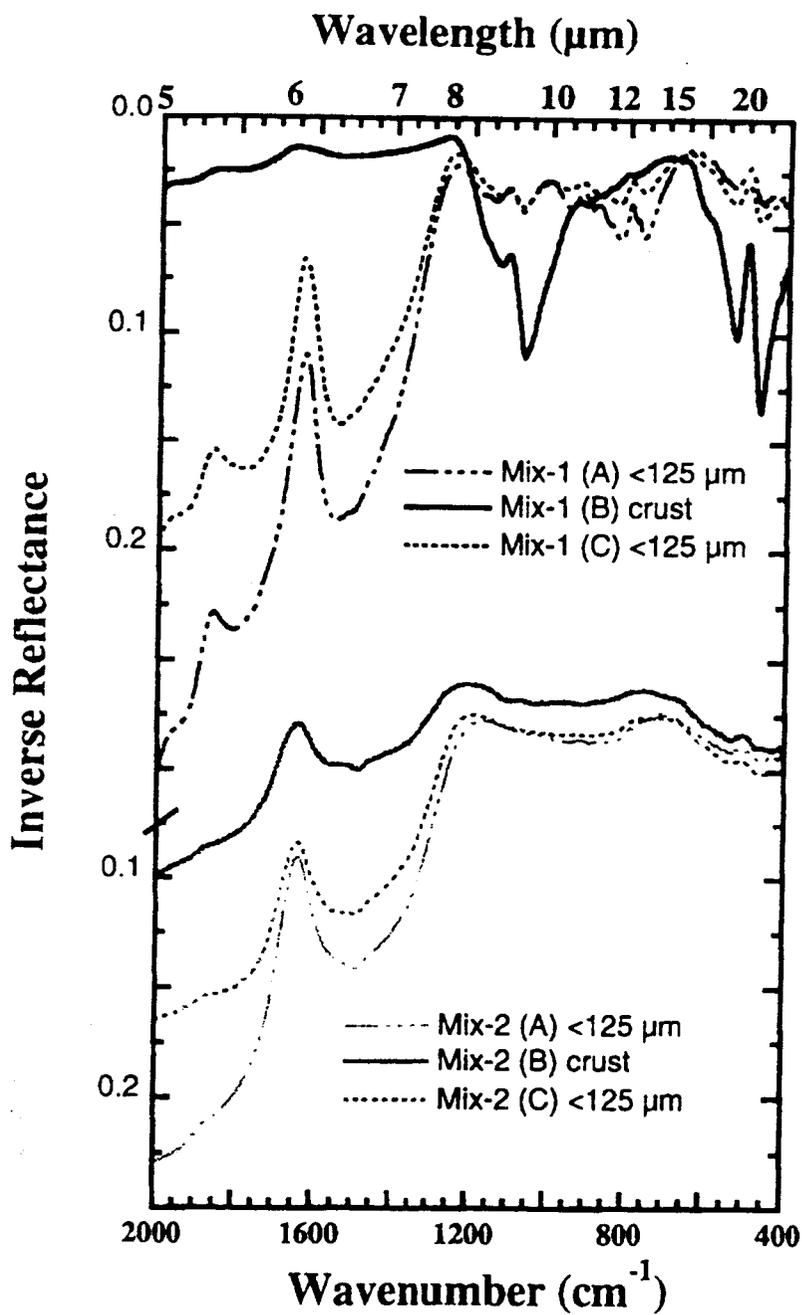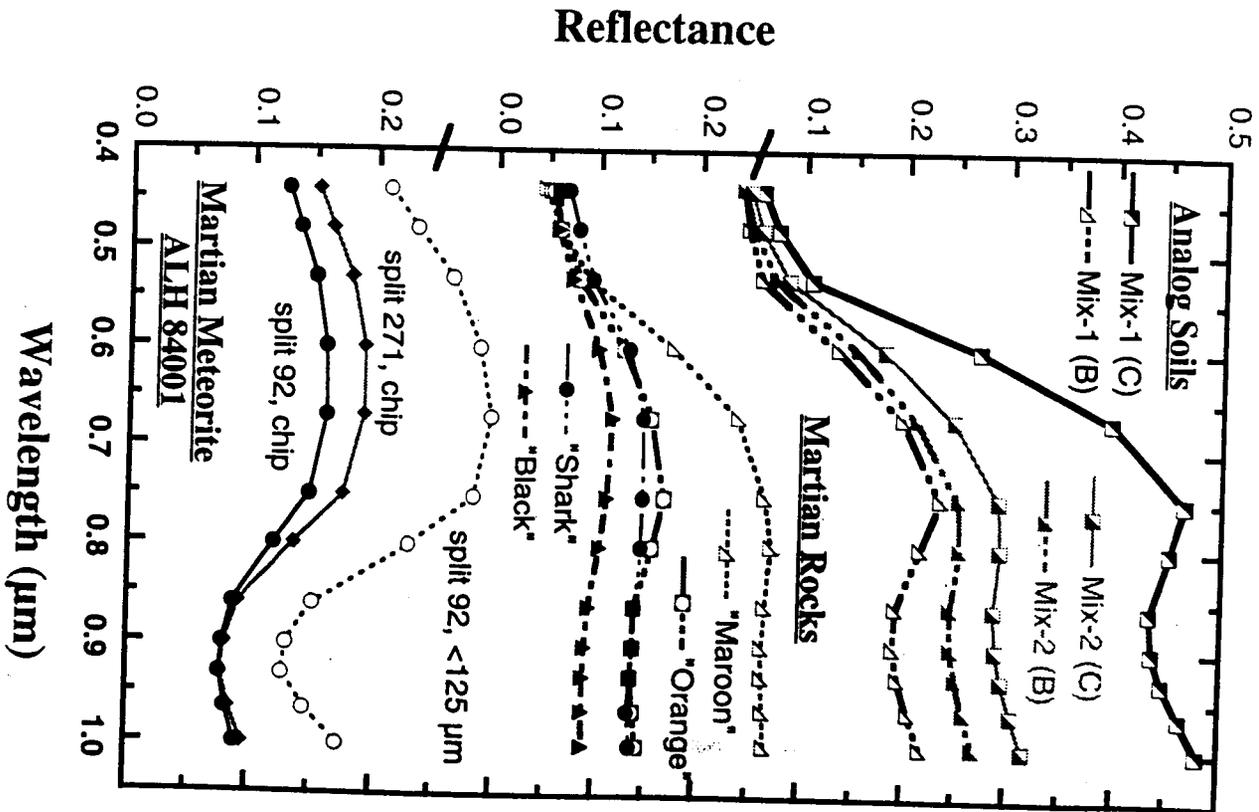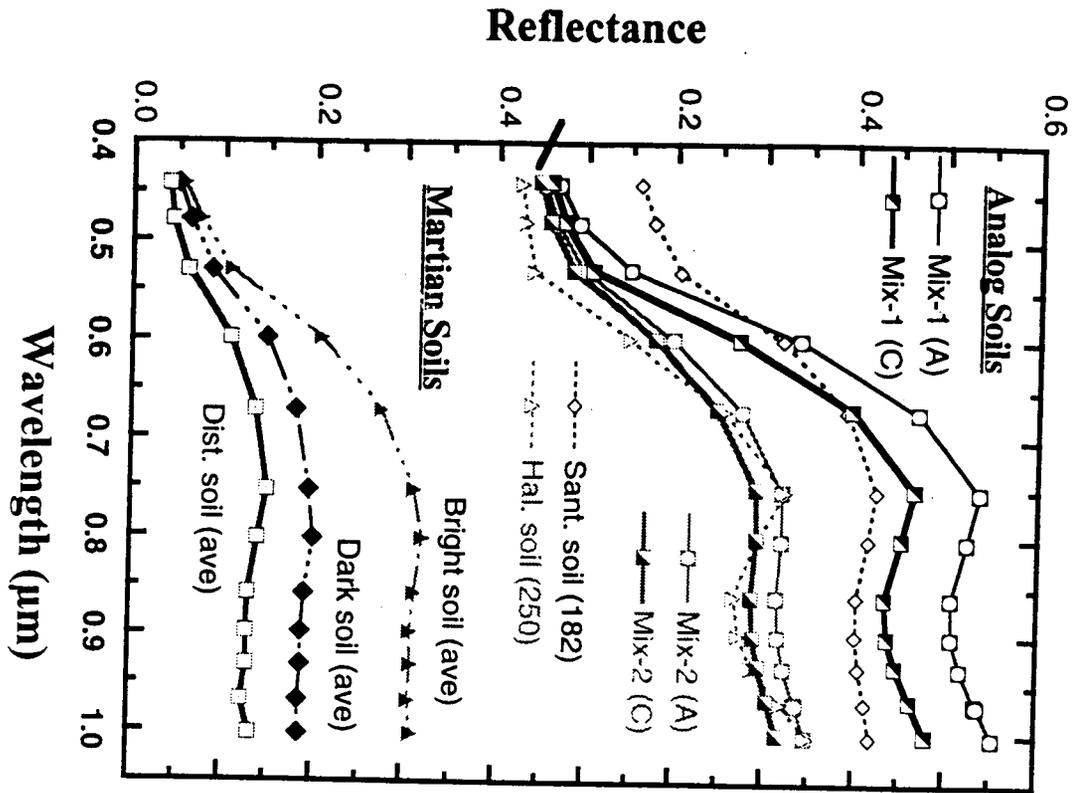
Plate 1

Images of Samples in Wet/Dry Cycling Experiments

| | 1. dried in desiccator | 2. H₂O added, air dried | 3. dried in desiccator | 4. H₂O added, desiccator |

Mix-1
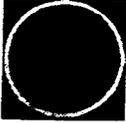
Fe-mont

Mix-2

Hal. soil

Plate 2

Drift and Cemented Soils